ION TRANSFER AND DOUBLE LAYER STUDIES

ACROSS

THE WATER/o-DICHLOROBENZENE INTERFACE

A Thesis Presented to the

School of Graduate Studies

Addis Ababa University

In Partial Fulfilment of the Requirements for

the Degree of Master of Science in Chemistry

A C K N O W L E D G E M E N T S

I am highly indebted to my advisors Dr. Theodros Solomon and Dr. B. Hundhammer, without whose constant help the research work as well as the preparation of the thesis would have been impossible.

I also wish to thank Dr. K. Base, Institute of Inorganic Chemistry, Czechoslovak Academy of Science, for the generous gift of CsDCC. I wish to express my deepest appreciation to W/o Senait Tadele who did her most in keeping up the moral and material need for the successfulness of my work.

I would also like to thank Ato Hassen Mohammed and Ato Beyene Erbeto, who contributed much to the materialization of this work. My thanks also go to Dr. Habtamu Zewdie, Ato Hailemichael Alemu and Dr. Eva Zena who were heartedly longing to see me successfully finish the research in time. I am also grateful to Ato Befekadu Regassa for typing the manuscript.

The Swedish Agency for Research Co-operation with Developing Countries (SAREC) is acknowledged for the financial assistance obtained through the Ethiopian Science and Technology Commission.

Table of Contents

List of Figures

5.

Page

List of Tables

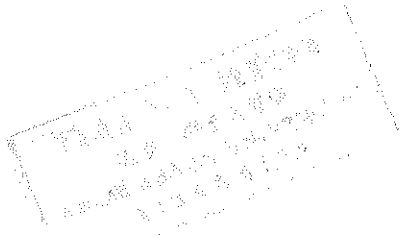

Abstract

Ion transfer across the water/o-dichlorobenzene interface has been investigated by ac cyclic voltammetry from the peak of which the half-wave potentials of the ion studied have been determined. The zero point on the $\Delta\Psi$-scale has been fixed using 10 mM PNPDCC saturated with TPAsTPB as a base electrolyte in o-DCB. A wide potential window has also been obtained by employing tetradodecylammonium dicarbollylcobaltate (III) (TDADCC), as supporting electrolyte in o-DCB. The values of the standard Galvani potential difference and the standard Gibbs energies of partition for individual ions in o-DCB have been evaluated taking into account ion association in o-DCB. The association constant of the base electrolyte in o-DCB has been determined from conductivity measurements. The standard Gibbs energies of partition for some ions in the water/o-DCB system have also been determined from solubility experiments. These have been compared with the values obtained from voltammetric experiments.

Preliminary studies on the electrical double layer across the water/o-DCB interface have been made using the impedance technique. The experimental interfacial capacitance have been compared with the theoretical diffuse layer capacitances calculated by the Gouy-Chapman theory.

1. INTRODUCTION

In recent years the electrochemical phenomena at liquid/liquid interface have attracted a great deal of interest due to the wide range of application of these systems in chemistry and biology. Although the investigation of the polarization of the interface between two immiscible electrolyte solutions (ITIES) is small in scope compared to the study of metal/electrolyte solution interface, studies of such system may be used to extend the field of analytical voltammetric methods and may serve as very simple membrane models. An ITIES may supply information in the studies of liquid membrane ion-selective electrode, bilayer lipid membranes, phase transfer catalysis and two-phase electrolysis, because charge transfer processes across the ITIES can be studied by standard electrochemical methods.

The properties of o-dichlorobenzene (ε =10.03, (20°C), ρ = 1.306 g cm^{-3}, η = 1.324 cp, solubility in water 2.7×10^{-3} mol l^{-1}, solubility of water in o-DCB 2.2×10^{-1} mol l^{-1}) make it a promising non-aqueous solvent for the studies of liquid/liquid interface. The purpose of the present work is to determine the standard Gibbs energies of ion transfer from water to o-dichlorobenzene, and hence the standard Galvani potential difference and the half-wave potentials of some ions between water and o-DCB (about which very little is known [35]) from voltammetric and

solubility experiments. The double layer capacitance data for the polarized water/o-DCB interface have not been so far reported. Hence the present work also include a preliminary study of double layer capacitance of the water/o-DCB interface in the presence of different electrolytes in each phase by ac impedance technique and a comparison of the experimental results with the theoretical capacitance of the interface calculated by the use of the Gouy-Chapman theory is made.

2. LITERATURE REVIEW

The first paper describing the electrical properties of the interface between two immiscible electrolyte solutions (ITIES) is the work done by Nernst and Riesenfeld (1) which dates back to 1902. Some time after the results of Nernst and Riesenfeld, research on ITIES was restricted to the study of equilibrium electrical potential differences between an aqueous and a non-aqueous phase in contact in the presence of various electrolytes. An exact thermodynamic treatment of the ITIES was obtained by Bonhoeffer et al, (2), and in more detail by Karpfen and Randels (3).

Gaustalla (4,5) observed changes in interfacial tension when an electric current was passed through the system of cetyltrimethylammonium bromide in water and in nitrobenzene. He thought that this effect is due to the electrical field arising at the electrode during current flow. He termed this effect electroadsorption. Using the Nernst-Riesenfeld approach, Blank (6) analysed the interfacial data and showed that the effect of electroadsorption is exclusively due to the accumulation or depletion of surface-active electrolyte at the interface. These studies also led to the discovery of mechanical interfacial movement. A similar approach was used by D'Epenoux

and Gavach (7,8) and also by Joos et al. (9, 10).

Electrochemical phenomena at the ITIES have been reviewed quite thoroughly by Koryta (11, 13, 14), and also by Koryta and Vanysek (15), by Vanysek and Buck (16), by Girault and Schiffrin (17) and by Vanysek (18).

The most extensively used experimental techniques in the ITIES studies are chronopotentiometry (19-21), polarography with electrolyte dropping electrode (22, 23), cyclic voltammetry (24-27) and impedance measurements (28). A new method for evaluation of the capacitance of ITIES and the overall ohmic potential drop is the fast performance galvanostatic pulse technique (29-31).

For electrochemical processes involving water/organic solvent systems, Koryta and Vanysek (15) have listed the following requirements for the choice of the non-aqueous solvent.

1. The organic solvent must dissolve only small amount of water, since otherwise the base electrolytes cannot be confined to their respective phases and no suitable potential range for polarization of the interface would be found.

2. The solvent should be sufficiently polar (with minimum relative permitivity of about 10) to safeguard sufficient conductivity of the non-aqueous phase.

3. Its density must differ considerably from water so that a stable interface could be formed.

Besides the well established non-aqueous solvents nitrobenzene and 1,2-dichloroethane, solvents like acetophenone (32), o-nitrophenyl ether (33), chloroform (34,35), o-nitrotoluene (34), benzonitrile (34, 36), dichloromethane (37), and nitroethane (38) have been used. In addition to these water/pure solvent systems, mixtures of solvents like nitrobenzene + chlorobenzene (39), nitrobenzene + benzene (40), and nitrobenzene + benzonitrile (32) have been used. A large number of organic solvents have been used by Kihara et al. (35) for the investigation of the half-wave potentials of ion transfer by the polarographic method.

The potential range where the transfer of individual ions can be investigated without interference of the transfer of the ions of the base electrolytes depends on the hydrophilicity of the ions of the base electrolyte in the aqueous phase and on the lipophilicity of the ions of the base electrolyte in the organic phase (11). These supporting electrolytes in the aqueous and organic solvents should have an appropriate solubility in each phase. And also they should be composed of ions that are stable and hardly transfer to the other phase. A wide potential window can be attained when the supporting electrolytes in the organic phase are composed of monovalent ions having large ionic radii. The ions

tetrabutylammonium (TBA^+) (11), tetraphenylborate (TPB^-) (11, 42), 3,3-como-bis (undecahydro-1,2-dicarba-3-cobalta-closododecarbor) ate(DCC^-) (42) and dipicrylaminate (DPA^-) (41) have been widely used as suitable components of the base electrolyte in the organic phase. In order to extend the potential window towards more negative potentials, tetraphenylarsonium ($TPAs^+$) (41), Crystal Violet (41, 45), and μ-nitrido-bis (triphenylphosphorus) (PNP^+) (42) ions have been employed.

For thermodynamic studies of ion transfer across the ITIES, standard Gibbs transfer energies or standard potential differences for single ions are not accessible to direct measurements, since they are always related to the corresponding quantity for another ion (43). Using the 'TPAs TPB assumption', which states that the anion and cation of TPAsTPB have equal standard Gibbs transfer energies between an arbitrary pair of solvents, Rais (44) and, Czapkiewicz and Czapkiewcz-Tutaj (46) evaluated standard Gibbs energy of ion transfer from water to nitrobenzene and from water to 1,2-dichloroethane respectively. The values of standard Gibbs energy of transfer of ions were compared with solubility data by Abraham et al. (47). The standard Gibbs energies of ion transfer between various solvents have been critically reviewed by Marcus (48).

Concerning double layer studies, the first quantitative treatment of the electrical double layer at the ITIES was conducted by Verwey and Niessen (as quoted in

For the double layerrstudies of ITIES, electrochemical cells with a planar or spherical liquid/liquid boundary have been in common use. Senda et al. (54) and Buck et al. (55) stressed that the flatness of the boundary and the geometric configuration of the four eleotrodes are of critical importance for ensuring the homogeneous polarization of the interface. The ohmic potential drop (the solution resistance) between the tip of the Luggin capillary and the point just outside the interfacial region on each side of the interface ban be compensated by means of positive feed back (53) and algebraic subtraction (29, 56) under the potentiostatic or galvanostatic conditions respectively. Brauzzi and Uhlken (57) have shown a new method of IR drop elimination by the application of a potentiostat based on a periodic current interuption to a four electrode system.

While the interfacial tension of the ITIES may be measured directly, the differential capacitance of the double layer at the ITIES has to be evaluated through a careful analysis of experimental data. Gavach et al. (58) used the drop-weight and Buck et al. (59) the maximum bubble pressure methods to measure the surface tension of the water/nitrobenzene interface in the presence of bromides of sodium and tetraalkylammonium ions in water and tetraalkylammonium tetraphenylborates in nitrobenzene. Comparison of the experimental surface charge densities with those calculated by the help of GC theory indicated

t

that the potential difference across an ITIES is concentrated in the diffuse double layer (58, 59). Kakiuchi and Senda (60, 61) measured, by the drop-weight/drop-time method, electrocapillary curves for the systems nitrobenzene solution of tetrabutylammonium tetraphenylborate(TBATPB) and aqueous solution of LiCl. Their results showed that the zero-charge potential difference was practically independent of the concentration of both the electrolytes. Girault and Shiffrin (62) conducted surface tension measurements of the interface between KCl in water and TBATPB in 1,2-dichloroethane. The values were in good agreement with the doubly integrated capacitance obtained from Galvanostatic pulse measurements.

The impedance of an ideally polarizable interface can be measured by means of alternating-current bridge (63) or phase selective detection (61, 63). The results were presented in the form of complex plane impedance. The high frequency semi-circle observed in some cases was shown (64) to be due to a capacitive coupling between the reference electrodes or was ascribed (50, 65) to the geometric bulk-phase capacitance. Recently Chechirlian et al. (66), through impedance measurements in low conductivity media, have shown that the conductivity of the media, the design of the reference electrode and the geometry of the cell all have a role in affecting impedance measurements at the high frequency limit.

Capacitance data have so far been reported for the water/nitrobenzene (51, 64) and water/1,2-dichloroethane (63,68) systems in the presence of different electrolytes by measuring the surface tension (50, 59, 61) and impedances (63, 64, 68).

3. THEORY

3.1. Equilibrium Conditions

For a system containing an ion i of charge z partitioned between two immiscible liquids, say α and β

$$i(\alpha) \rightleftharpoons i\ (\beta)$$

the equilibrium condition is that the electrochemical potential $\tilde{\mu}_i$ of the ion in the two phases must be equal.

$$\tilde{\mu}_i\ (\alpha) = \tilde{\mu}_i(\beta) \qquad (3.1.1)$$

or

$$\mu_i^{\circ}(\alpha) + RT\ln a_i(\alpha) + z_iF\varphi_i(\alpha) = \mu_i^{\circ}(\beta) + RT\ln a_i(\beta) + z_iF\varphi_i(\beta) \qquad (3.1.2)$$

where $\mu_i^{\circ}(\alpha)$ and $\mu_i^{\circ}(\beta)$ are the standard chemical potentials, $a_i(\alpha)$ and $a_i(\beta)$ are activities and $\varphi_i(\alpha)$ and $\varphi_i(\beta)$ are inner potentials of the ion in the phases α and β.

The inner potential difference between the two phases can be obtained from a rearrangement of equation (3.1.2)

$$\Delta_{\beta}^{\alpha}\varphi = \varphi_i(\alpha) - \varphi_i(\beta) = \frac{\mu_i^{\circ}(\beta) - \mu_i^{\circ}(\alpha)}{z_iF} + \frac{RT}{z_iF}\ln\frac{a_i(\beta)}{a_i(\alpha)} \qquad (3.1.3)$$

or

$$\Delta_{\beta}^{\alpha}\varphi_i = \Delta_{\beta}^{\alpha}\varphi_i^{\circ} + \frac{RT}{z_iF}\ln\frac{a_i(\beta)}{a_i(\alpha)} \qquad (3.1.4)$$

where $\Delta_{\beta}^{\alpha}\varphi_i^{\circ} = \left[\mu_i^{\circ}(\beta) - \mu_i^{\circ}(\alpha)\right]/z_iF = -\Delta G_{t,i}^{\circ,\alpha\rightarrow\beta}/z_iF$ (3.1.5)

$\Delta\varphi_i^{\circ}$ is the standard Galvani potential difference between the phases α and β. It is defined as the equilibrium value of the Galvani potential difference $\Delta\varphi_i$, at unit ratio of ion activities $a_i(\beta)$ and $a_i(\alpha)$. $\Delta G_{t,i}^{\circ,\alpha\rightarrow\beta}$ is the

standard Gibbs energy of transfer of ion i from solvent α to solvent β.

Provided that the standard Galvani potential difference can be obtained experimentally (from voltammetry or chronopotentiometry), the standard Gibbs energies of transfer of ions can be calculated from eqn. (3.1.5).

The transfer of ions across ITIES studied by dc cyclic voltammetry follow formally the same laws as those governing electron transfer at the metal/electrolyte solution interface. At low sweep rates, ion transfer is diffusion controlled, and hence the current response of the system to a triangular potential signal can be treated in the same way as a reversible electron transfer reaction (69). Hence the current potential relationship is given by

$$i = z^{3/2} FAC_i^b (D_i VII)^{\frac{1}{2}} x(at) \qquad (3.1.6)$$

where A is the area of the interface, c_i^b is the bulk concentration, v is the sweep rate, D_i is the diffusion coefficient and x(at) is a current function (69).

The peak potential of ion transfer $\Delta_\beta^\alpha \varphi_{p,i}$ obtained from the cyclic dc voltammogram is related to the polarographic half-wave potential $\Delta \varphi_{\frac{1}{2},i}$ at 25°C by the relation

$$\Delta \varphi_{p,i} = \Delta \varphi_{\frac{1}{2},i} \pm 0.0285/z \qquad (3.1.7)$$

The (+) sign stands for the positive current and the (-) sign stands for the negative current potentials. The $\Delta \varphi_{\frac{1}{2},i}$ in turn is related to the standard Galvani potential difference by the equation:

$$\Delta^{\alpha}_{\beta}\varphi_{\frac{1}{2},i} = \Delta^{\alpha}_{\beta}\varphi^{o}_{i} + \frac{RT}{2zF}\ln\frac{D_i(\alpha)}{D_i(\beta)} + \frac{RT}{zF}\ln\frac{\gamma_i(\beta)}{\gamma_i(\alpha)} \qquad (3.1.8)$$

Taking ion association into account in the organic phase (for low dielectric permitivity organic solvents) equation (3.1.8) is written as:

$$\Delta\varphi_{\frac{1}{2},i} = \Delta\varphi^{o}_{i} + \frac{RT}{2zF}\ln\frac{D_i(w)}{D_i(o)} + \frac{RT}{zF}\ln\frac{\gamma_i(o)}{\gamma_i(w)} - \frac{RT}{zF}\ln\left\{1+K_A C_o \alpha \left(\frac{D_A(o)}{D_i(o)}\right)^{\frac{1}{2}}\right\} \qquad (3.1.9)$$

where C_o and α are the analytical concentration and degree of dissociation of the supporting electrolyte in the organic phase respectively. K_A is the association constant of the ion investigated with the respective counter ion of the supporting electrolyte, D_i and D_A are the diffusion coefficients of the ion transfered and the associated ion in the organic phase respectively. $\gamma_{\pm}(w)$ and $\gamma_{\pm}(o)$ are the mean activity coefficients of the ion in the respective phases.

The half-wave potential difference $\Delta\varphi_{\frac{1}{2},i}$, can also be obtained from ac cyclic voltammetric experiments using the theory of ac cyclic voltammetry (70). According to this theory, for completely reversible ion transfer processes the forward and reverse ac scans should yield overlapping peaks in the plot i(wt)vvs $\Delta\varphi_{dc}$, passing through a maximum at $\Delta\varphi_{\frac{1}{2}}$. Furthermore, the half-peak width should be 90 mV regardless of the sweep rate if the system behaves reversibly.

3.2. Non-Polarizable Interface

A non-polarizable interface is formed between two immiscible solvents α and β when a single binary electrolyte MA, is dissolved in both phases. The system can be represented as (15):

$$\begin{matrix} M^+A^- \\ (\alpha) \end{matrix} \Big\| \begin{matrix} M^+A^- \\ (\beta) \end{matrix} \qquad (3.2.1)$$

where the perpendicular strokes represent the interface.

The Galvani potential difference between phases α and β is given by (71):

$$\Delta\Psi = \left[\mu^\circ_{M^+}(\beta) - \mu^\circ_{M^+}(\alpha)\right]/F + RT/F \ln\left[a_{M^+}(\beta) \,/\, a_{M^+}(\alpha)\right] \qquad (3.2.2)$$

$$= \left[\mu^\circ_{A^-}(\beta) - \mu^\circ_{A^-}(\alpha)\right]/F - RT/F \ln\left[a_{A^-}(\beta) \,/\, a_{A^-}(\alpha)\right] \qquad (3.2.3)$$

After adding the two equations and dividing by 2 we get

$$\Delta\Psi = \frac{\Delta\Psi^\circ_{M^+} + \Delta\Psi^\circ_{A^-}}{2} + \frac{RT}{2F} \ln \frac{a_{M^+}(\beta)\, a_{A^-}(\alpha)}{a_{M^+}(\alpha)\, a_{A^-}(\beta)} \qquad (3.2.4)$$

substitution of (Cγ) for the activity results:

$$\Delta\Psi = \frac{\Delta\Psi^\circ_{M^+} + \Delta\Psi^\circ_{A^-}}{2} + \frac{RT}{2F} \ln \frac{\gamma_{M^+}(\beta)\, \gamma_{A^-}(\alpha)}{\gamma_{M^+}(\alpha)\, \gamma_{A^-}(\beta)} \qquad (3.2.5)$$

where γ's are the activity coefficients of the species in the respective phases.

3.3. Ideally Polarizable Interface

As shown by Koryta et al. (11), a system can behave as an ideally polarizable interface when two different electrolytes M_1A_1 and M_2A_2 are dissolved in two immiscible liquids α and β respectively. It can be represented as

$$\begin{matrix} M_1A_1 \\ (\alpha) \end{matrix} \Big\| \begin{matrix} M_2A_2 \\ (\beta) \end{matrix} \qquad (3.3.1)$$

This is possible when the electrolytes have the property that the standard Gibbs energies of transfer for the ions M_1^+ and A_1^- from phase α to phase β are large and positive ($\Delta G_{t,M_1^+}^{o,\alpha\to\beta}$ and $\Delta G_{t,A_1^-}^{o,\alpha\to\beta} \gg 0$) and the opposite is true for ions M_2^+ and A_2^- ($\Delta G_{t,M_2^+}^{o,\alpha\to\beta}$ and $\Delta G_{t,A_2^-}^{o,\alpha\to\beta} \ll 0$). The Galvani potential difference $\Delta\varphi$, between the two phases is determined by the charge at the interface which is supplied from an external source, but not by the activity of the ions.

3.4. Ionic Standard Gibbs Energies of Transfer

For a salt MA distributed between two phases α and β

$$M^+(\alpha) + A^-(\alpha) \rightleftharpoons M^+(\beta) + A^-(\beta) \qquad (3.4.1)$$

The standard Gibbs energy of transfer of the salt M^+A^- from α to β is given by (17):

$$\Delta G_{t,MA}^{o,\alpha\to\beta} = \left[\mu_{M^+}^{o}(\beta) + \mu_{A^-}^{o}(\beta)\right] - \left[\mu_{M^+}^{o}(\alpha) + \mu_{A^-}^{o}(\alpha)\right] \qquad (3.4.2)$$

The standard Gibbs energy of transfer of the salt, $\Delta G_{t,MA}^{o,\alpha\to\beta}$, is a thermodynamically measurable quantity that can be obtained from the difference in energies of solvations of the salt MA between solvent α and solvent β. It is also equal to the sum of the standard Gibbs energies of transfer of the cation and anion of the salt, i.e.

$$\Delta G_{t,MA}^{o,\alpha\to\beta} = \Delta G_{t,M^+}^{o,\alpha\to\beta} + \Delta G_{t,A^-}^{o,\alpha\to\beta} \qquad (3.4.3)$$

where the standard Gibbs energies of transfer of the ions are given by:

$$\Delta G_{t,i}^{o,\alpha\to\beta} = \mu_i^{o}(\beta) - \mu_i^{o}(\alpha) \qquad (3.4.4)$$

However, $\Delta G_{t,i}^{o,\alpha\to\beta}$ of individual ions are not accessible to a direct measurement. To make their quantitative

measurement possible an extra thermodynamic assumption must be made. Of the many different assumptions (73), the "tetraphenylarsonium tetraphenylborate (TPAsTPB) assumption" is widely used. This states that standard Gibbs energies of transfer of $TPAs^+$ cation and TPB^- anion are equal for any pair of solvents. These ions are symmetrical species of much of the same size and shape so that the charge is buried under the phenyl groups. From this assumption we have:

$$\Delta G^{o,\alpha\rightarrow\beta}_{t,TPAs^+} = \Delta G^{o,\alpha\rightarrow\beta}_{t,TPB^-} = \tfrac{1}{2}\Delta G^{o,\alpha\rightarrow\beta}_{t,TPAsTPB} \qquad (3.4.5)$$

On the basis of this assumption a scale for standard Gibbs energies of transfer of ions from one solvent to another can be obtained. For example the standard Gibbs energy of transfer for chloride ion can be determined from partition experiments by determining $\Delta G^{o,\alpha\rightarrow\beta}_{t,TPAsTPB}$ and $\Delta G^{o,\alpha\rightarrow\beta}_{t,TPAsCl}$ between the two solvents. The value for the chloride ion transfer can be obtained from the relation:

$$\Delta G^{o,\alpha\rightarrow\beta}_{t,Cl^-} = \Delta G^{o,\alpha\rightarrow\beta}_{t,TPAsCl} - \tfrac{1}{2}\Delta G^{o,\alpha\rightarrow\beta}_{t,TPAsTPB} \qquad (3.4.6)$$

Again from the same assumption the standard Galvani potential difference for individual ions $\Delta\phi^o_i$, can be calculated from equation (3.1.5).

For voltammetric studies of ion transfer processes, the TPAsTPB assumption can be employed for fixing the absolute value of the Galvani potential difference of ions. If TPAsTPB is used as a base electrolyte in the organic phase and Li_2SO_4 or LiCl in the aqueous phase,

the voltammogram will be limited at the negative potential by the transfer of $TPAs^+$ cation from the organic phase to water and, at the positive potentials, the voltammogram will be limited by the transfer of TPB^- anion from the organic phase to water. The zero point of the potential scale is then fixed (see Ref. 33).

$$\frac{\Delta^{\alpha}_{\beta} E_{\frac{1}{2}}(TPAs^+) + \Delta^{\alpha}_{\beta} E_{\frac{1}{2}}(TPB^-)}{2} = \Delta\phi = 0 \qquad (3.4.7)$$

Theoretically $\Delta G^{0,\alpha\to\beta}_{t,i}$ can be calculated by taking the difference in the standard Gibbs energy of solvation and hydration in the organic (β) and aqueous (α) solvents using the relation (74).

$$\Delta G^{0,\alpha\to\beta}_{t,i} = \Delta G^{0}_{s,i} - \Delta G^{0}_{h,i} \qquad (3.4.8)$$

where $\Delta G^{0}_{s,i}$ is the standard Gibbs energy of solvation and $\Delta G^{0}_{h,i}$ is the standard Gibbs energy of hydration of the ion i. The standard free energies of solvation of a salt can be obtained from solubility experiments using the relation:

$$\Delta G^{0}_{s} = -RT\ln K_{sp} \qquad (3.4.9)$$

$$\text{where } K_{sp} = (C_o\alpha)^2\gamma_{\pm}^2 \qquad (3.4.10)$$

The standard Gibbs energy of solvation ΔG^{0}_{s}, can be split in to an electrical contribution ΔG^{0}_{e}, and a neutral contribution ΔG^{0}_{n} (74,75).

$$\Delta G^{0}_{s} = \Delta G^{0}_{e} + \Delta G^{0}_{n} \qquad (3.4.11)$$

The neutral contribution ΔG^{0}_{n}, is defined as the Gibbs energy of solvation of a non-polar gaseous solute of the same size as the ion considered.

The electrical contribution can be calculated using a one-layer solvation model in which an ion of crystallographic radius a and dielectric constant unity is surrounded by a layer of solvent of thickness (b-a) and dielectric constant ϵ_1, and immersed in a bulk solvent of dielectric constant ϵ_o. The electrical contribution is given by (17)

$$\Delta G_e^o = \frac{N(ze)^2}{8\pi\epsilon_o}\left(\frac{1}{\epsilon_1}-1\right)\left(\frac{1}{a}-\frac{1}{b}\right) + \left(\frac{1}{\epsilon_o}-1\right)\frac{1}{B} \qquad (3.4.12)$$

The radius of the solvent molecule calculated from the bulk molar solvent volume ($\bar{v}$) using the Stearn-Eyring formula $r^3 = \bar{v}/8N$, can be taken as the thickness of the solvent layer b-a while the dielectric constant ϵ_1 of this solvent is taken to be 2 for all organic solvents.

The neutral term is expressed as a first-order polynomial of the ionic radius (75)

$$\Delta G_n^o = ma + c \qquad (3.4.13)$$

where m and c are constants, the values of which for several solvents are known (75).

The standard Gibbs energies of transfer of ions described above refers to the transfer of ions from the pure solvent α to the pure solvent β. It is different from the standard Gibbs energy of partition $\Delta G_{p,MA}^{o,\alpha\rightarrow\beta}$, which refers to the transfer of ions from the solvent α saturated with β to the solvent β saturated with α. The latter is given by:

$$\Delta G_{p,MA}^{o,\alpha\rightarrow\beta} = \left[\mu_M^o{}^+(\beta sat) + \mu_A^o{}^-(\beta sat)\right] - \left[\mu_M^o{}^+(\alpha sat) + \mu_A^o{}^-(\alpha sat)\right]$$
$$= -RT\ln P_{MA}^{\alpha,\beta} \qquad (3.4.14)$$

where $P_{M\Lambda}^{\alpha,\beta}$ is the partition coefficient given by:

$$P_{M\Lambda}^{\alpha,\beta} = \frac{a_{M^+}(\beta sat)\, a_{\Lambda^-}(\beta sat)}{a_{M^+}(\alpha sat)\, a_{\Lambda^-}(\alpha sat)} \qquad (3.4.15)$$

In the case of solvents of low miscibility, the ionic standard Gibbs energy of transfer is equal to the ionic standard Gibbs energy of partition showing that ions are not hydrated in the organic phase (17).

3.5. Ion Association

Calculations of standard free energies of solvation ΔG_s^o, in low dielectric non-aqueous solvents through solubility measurements have some technical difficulties, because the electrolyte in such solvents will be dissolved not as a pair of ions but also as ion pairs $M^+\Lambda^-$. Therefore the values of the association constant K_Λ, for the equilibrium:

$$M^+(solv) + \Lambda^-(solv) \rightleftharpoons M^+\Lambda^-(solv) \qquad (3.5.1)$$

must be known or capable of being estimated. If the stoichiometric concentration of $M^+\Lambda^-$ is C and its degree of dissocition α, then K_Λ is given by:

$$K_\Lambda = \frac{(1-\alpha)C}{(\alpha C \gamma_\pm)^2} = \frac{(1-\alpha)}{\alpha^2 C \gamma_\pm^2} \qquad (3.5.2)$$

where $\gamma_\pm$ is the mean molar activity coefficient which is unity for the undissociated molecule or associated ions.

The simplest theoretical evaluation of K_Λ, which is also an operational definition for the undessociated molecule or ion-pair, considers as paired only ions in actual contact, that is those whose centers are exactly

a distance of mean ionic diameter apart (76). Another approach (Bjerrum's treatment), which broadens the concept of ion-pairs, is to include not only ions in contact, but also oppositely charged ions separated by one or more solventsmolecules (solvent-shared and solvent-separated ion-pairs) whose mutual interaction energy is greater than $2kT$, where $2kT$ is an arbitrary limit for defining association. It is given by:

$$2kT = \frac{|z+z_-|e_o^2}{\varepsilon a} \qquad (3.5.3)$$

where k is the Botlzman constant, z is the charge of the ions, e is the elementary charge, ε is the dieleotrio constant of the solvent a is the mean ionic diameter and T is absolute temperature.

The association constant K_A can be estimated using the assumption $\alpha = \Lambda/\Lambda_o$ and the relation deduced by Arhenius and Ostwald (sited in Ref. 77).

$$\frac{1}{\Lambda} = \frac{1}{\Lambda_o} + \frac{c\Lambda K_A}{\Lambda_o^2} \qquad (3.5.4)$$

where Λ_o is equivalent conductance at infinite dilution, α is the degree of dissociation and c is concentration of the electrolyte in equivalents per liter of solution. The plot of $\frac{1}{\Lambda}$ vs $c\Lambda$ can be used to obtain approximate value for both Λ_o and K_A. From the intercept $1/\Lambda_o$ is obtained and from the slope K_A/Λ_o^2 is obtained.

A better equation for determining the association constant from conductivity measurement, which is a modification of the Arhenius-Ostwald equation (3.5.4) is the one that is proposed by Shedlovsky (sited in Ref. 77).

$$\frac{1}{\Lambda S(z)} = \frac{K_\Lambda C \Lambda \gamma_\pm^2 s(z)}{\Lambda_o^2} + \frac{1}{\Lambda_o} \qquad (3.5.5)$$

where $s(z)$ is the Shedlovsky function given by:

$$s(z) = \left[\frac{z}{2} + \sqrt{1+\left(\frac{z}{2}\right)^2}\right]^2 \qquad (3.5.6)$$

and $$z = s\,\Lambda_o^{3/2}(C\Lambda)^{\frac{1}{2}} \qquad (3.5.7)$$

s is the Onsanger coefficient given by:

$$s = \alpha\Lambda_o + 3\beta \qquad (3.5.8)$$

where, $\alpha = \frac{0.8204\times10^6}{(\varepsilon T)^{3/2}}$ and $\beta = \frac{82.501}{\eta(\varepsilon T)^{\frac{1}{2}}}$ (3.5.9)

where ε and η are the dielectric constant and the viscosity of the solvent respectively. T is the absolute temperature, and $\gamma_\pm$ is the mean activity coefficient which can be calculated by successive approximation from the extended Debye-Huckel theory and making use of the association constant estimated from Eqn. (3.5.4)

3.6. Capacitance of Water/Organic Solvent Interface

Using the MVN model Fig. 3.1 (31), the Galvani potential difference $\Delta_o^w\varphi$, between two phases, water(w) and organic (o), in contact may be written in terms of the inner layer and diffuse layer contributions.

$$\Delta_o^w\varphi = \varphi(w) - \varphi(o) = \Delta_o^w\varphi_i + \varphi_{i2}(o) - \varphi_2(w) \qquad (3.6.1)$$

where $\varphi(w)$ and $\varphi(o)$ are electrical potentials in the bulk of water and organic phases respectively. $\Delta_o^w\varphi_i$ is the potential difference across the inner layer, and is given by: $\Delta_o^w\varphi_i = \varphi(x_2^w) - \varphi(x_2^o)$ (3.6.2)

$\varphi_2(w)$ and $\varphi_2(o)$ are the potential drops across the space charge regions (diffuse layer) in the phases water and organic respectively and are given by:

$$\varphi_{i2}(w) = \varphi(x_2^w) - \varphi(w) \text{ and } \varphi_{i2}(o) = \varphi(x_2^o) - \varphi(o) \qquad (3.6.3)$$

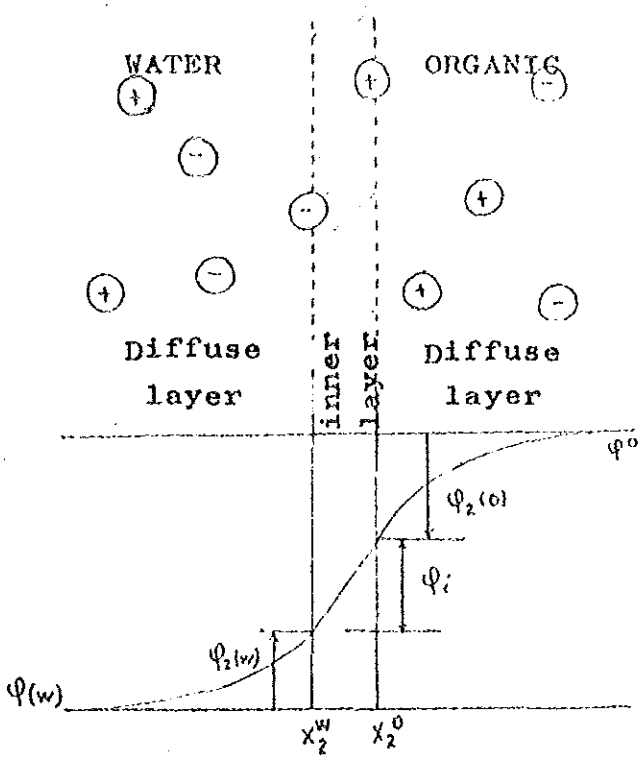

Figure 3.1. The Modified Verwey-Niessen Model of an ITIES. Full circles represent the point charge ions, and x_2^w and x_2^o are positions of ions in planes of closest approach (outer Helmholtzplane). Taken from Ref. (43).

from the electroneutrality condition $q(w) = -q(o)$ where $q(w)$ and $q(o)$ are surface charge densities in the aqueous and organic side of the interface respectively.

In the absence of ionic adsorption in the compact layer, the capacitance C, of the double layer is given by:

$$C = dq(w)/d\Delta_o^w\varphi \qquad (3.6.4)$$

upon differentiating Eqn. (3.6.1) with respect to the surface charge density:

$$\frac{d(\Delta_o^w\varphi)}{dq(w)} = \frac{d(\Delta_o^w\varphi_i)}{dq(w)} + \frac{d\varphi_2(o)}{dq(w)} - \frac{d\varphi_2(w)}{dq(w)} \qquad (3.6.5)$$

$$\bar{C}^{-1} = C_i^{-1} + C_d^{-1} \qquad (3.6.6)$$

where C_i is the inner layer capacitance and C_d is the diffuse layer capacitance given by:

$$C_d^{-1} = C_{2,o}^{-1} - C_{2,w}^{-1} \qquad (3.6.7)$$

Using the GC theory for a symmetrical electrolytes the surface charge densities are given by:

$$\begin{aligned} q(w) &= -2A^w \sinh(zF\varphi_2(w)/2RT) \\ q(o) &= -2A^o \sinh(zF\varphi_2(o)/2RT) \end{aligned} \qquad (3.6.8)$$

and consequently

$$\begin{aligned} C_{2,w} &= -\frac{\partial q(w)}{\partial \varphi_2(w)} = \frac{zFA}{RT}\cosh(zF\varphi_2(w)/2RT) \\ C_{2,o} &= -\frac{q(o)}{\partial \varphi_2(o)} = \frac{zFA}{RT}\cosh(zF\varphi_2(o)/2RT) \end{aligned} \qquad (3.6.9)$$

where $A^{w(o)} = (2RT\varepsilon^{w(o)}C^{w(o)})^{\frac{1}{2}}$

When a potential drop is applied across the interface, and assuming that $\Delta_o^w\varphi_i = 0$, the potential drop across the the aqueous diffuse layer can be calculated using the equation (72)

$$\varphi_2(w) = \frac{RT}{F}\left[\frac{(\varepsilon_w C_w)^{\frac{1}{2}} + (\varepsilon_o C_o)^{\frac{1}{2}}\exp(F\varphi_{app}/2RT)}{(\varepsilon_w C_w)^{\frac{1}{2}} + (\varepsilon_o C_o)^{\frac{1}{2}}\exp(-F\varphi_{app}/2RT)}\right] \qquad (3.6.10)$$

Where in the electric count t, C is the l

where ε is the dielectric constant, C is the bulk concentration of the respective phases, and φ_{app} is the applied potential drop across the interface.

The expression for the organic phase would be:

$$\varphi_{2}(o) = \varphi_{app} - \varphi_{2}(w) \qquad (3.6.11)$$

3.7. Equivalent Circuit of a Cell

A typical equivalent circuit for polarizable water/organic solvent interface can be represented as:

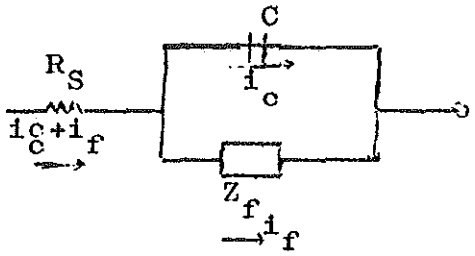

(3.7.1

where R_S solution resistance, C capacitance of the interface, and Z_f is faradaic impedance, i_c and i_f are double layer charging and faradaic currents respectively. The parallel elements are introduced because the total current passing through the interface is the sum of direct contributions from the faradaic process i_f and the double layer charging i_c. The faradaic process must be considered as a general impedance Z_f. Ofcourse all the current must pass through the uncompensated solution resistance, and hence R_S is inserted as a series element.

Since ion transfer is rather fast process, the faradaic impedance Z_f can be replaced by the Warburg impedance Z_w which corresponds to the diffusion-controlled process, Under this condition the real Z' and imaginary Z'' components of the complex impedance Z become (68)

$$Z' = |Z| \cos\delta = R_s + Z_c X \left[(X+1)^2+1\right]^{-1} \qquad (3.7.2)$$

$$Z'' = |Z| \sin\delta = Z_c X(X+1)/[(X+1)^2+1] \qquad (3.7.3)$$

where $X = (Z_w/Z_c)\sqrt{2}^{-1}$ and $Z_c = (WC)^{-1}$ (3.7.4)

If $X \gg 1$ (at high frequencies)

$$Z' = R_s + Z_c X^{-1} = R_s + (2C^2\sigma)w \qquad (3.7.5)$$

and $Z'' = Z_c$, where σ is a characteristic parameter of the faradaic process.

In this case there is a rather complicated relationship between Z" and Z' and the impedance is very informative.

If $X \ll 1$ (near the low frequency limit)

$$Z' = R_s + Z_w\sqrt{2} \text{ and } Z'' = Z' - R_s. \qquad (3.7.6)$$

The impedance plot is a straight line with slope 1. Using The interfacial capacitance C, can be evaluated from the slope of the plot of Z_c^{-1} vs w at a chosen potential E.

The phase shift between the applied and measured signal, δ can be calculated from the relation:

$$\delta = \tan^{-1}[i(90^\circ)/i(0^\circ)] \qquad (3.7.7)$$

The complex impedance Z, can be calculated from the inphase $i(0^\circ)$, and out of phase $i(90^\circ)$, components of the sinusoidal current flowing through the interface according to the relationship (29)

$$|Z| = \frac{V_o}{i^2(0^\circ) + i^2(90^\circ)^{\frac{1}{2}}} \qquad (3.7.8)$$

where V_o is the amplitude of the sinusoidal voltage.

4. EXPERIMENTAL

4.1. Chemicals and Preparation of Reagents

Acetone (Riedel-de Haen), n-propanol (B D H), Li_2SO_4 monohydrate (Merck), LiCl (Fluka 98%), LiF (BDH), $KMnO_4$ (M&B Laboratory Chemicals), $KClO_3$ (BDH), KNO_3 (Analar, BDH), KBF_4 (Hopkin & Williams), NH_4SCN (Analar, BDH), sodium picrate (BDH), NH_4PF_6 (Merck), tetrabutylammonium tetraphenylborate (TBATPB) (Fluka) were used as such without further purification.

o-Dichlorobenzene (Riedel-de-Haen) was distilled under reduced pressure and the middle half of the distillate was used. In all experiments doubly distilled water was used.

μ-Nitrido-bis(triphenylphosphorus)-3,3-commo-bis (undecahydro-1,2-dicarba-3-cobalta-closododecarbor)ate, (PNPDCC), was prepared by mixing equimolar acetone solution of PNPCl (Fluka) and CsDCC. The white precipitate of CsCl was filtered off. The acetone from the filtrate was evaporated under reduced pressure. The yellow solid, PNPDCC left was recrystallized twice from n-propanol. CsDCC was the generous gift from Dr. K. Base, Institute of Inorganic Chemistry, Czechoslovak Academy of Science.

Tetraphenylarsonium tetraphenylborate (TPAsTPB) was prepared by mixing equimolar aqueous solutions of TPAsCl (Fluka) and NaTPB (Fluka). The white precipitate formed was washed several times with water and recrystallized from acetone.

Tetradodecylammonium 3,3-como-bis(undecahydro-1,2-dicarba-3-cobalta-closododecarbor)ate (TDADCC) was prepared by mixing equimolar amounts of TDABr (Fluka) with CsDCC both dissolved in acetone. The precipitate of CsBr was filtered off and the crude orange product was obtained after evaporating the solvent. It was recrystallized twice from methanol.

Li_2SO_4, LiCl and LiF were used independently as base electrolytes in the aqueous phase while PNPDCC and TDADCC were veriously used as base electrolytes in the organic phase. TBATPB, tetraphenylphosphonium tetraphenylborate TPPTPB, (prepared by the same procedure used for the preparation of TPAsTPB) and TPAsTPB were used for solubility experiments. TPAsTPB was also used for fixing the zero point of the Galvani potential difference. Due to the low solubility of TPAsTPB in o-DCB, 10 mM solution of PNPDCC in o-DCB, saturated with TPAsTPB was used as a base electrolyte in the organic phase for fixing the zero point. Water and o-DCB were mutually saturated before preparing the solutions.

For the determination of the solubilities of the salts in o-DCB, an excess of each salt was dissolved in about 50 ml of water-saturated o-DCB and was shaken thoroughly at 25°C for several days. The mixtures were then allowed to settle and filtered. The filtrates were evaporated in an oven under reduced pressure to a constant weight. The standard Gibbs energies of solvation were calculated from the Equns. (3.4.9) and (3.4.10).

4.2. Cell Arrangement

The electrochemical cell which was employed for the studies is shown in Figure 4.1. The cell consisted of a glass vessel in which was put the aqueous phase; this was attached to a teflon body containing the organic phase. The interface was formed at the point of contact of the aqueous and organic phases. The cell had an interfacial area of 0.69 cm^2. A U-shaped glass capillary tube filled partially with the organic phase and part of it with an aqueous solution of R^+Cl^- (where R^+ is the cation of the base electrolyte in the organic phase) was inserted from the bottom into the teflon body close to the interface. This capillary served as a reference electrode in the organic phase.

The cell contained four electrodes. Two electrodes RE(w) and RE(o) served as reference electrodes for controlling the potential difference at the interface. They were immersed as closely as possible to each side of the interface to minimize iR drop of the system. Two platinium electrodes CE(w) and CE(o) served as current supplying and withdrawing electrodes (counter electrodes) while Ag/AgCl,sat.KCl, was used as a reference electrode in both phases.

4.3. Electronic Set Up

The block diagram of the electronic set up used for both dc and ac voltammetric measurements is shown in Figure 4.2. A four-electrode potentiostat (constructed and made available in the laboratory by Dr. B. Hundhammer)

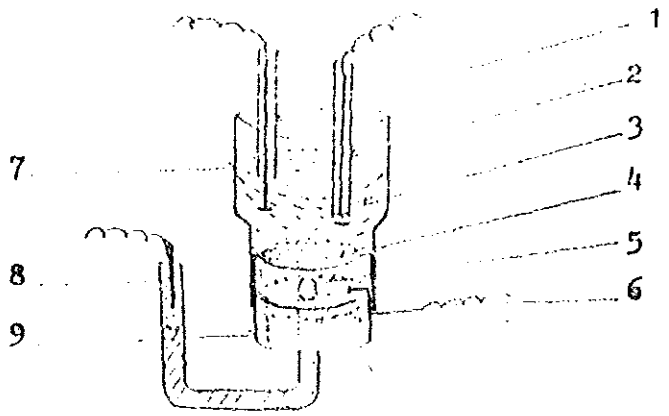

Figure 4.1 The Electrochemical cell employed in the study.

1. Counter electrode (water phase)
2. Reference electrode (water phase)
3. Aqueous phase
4. The interface
5. Organic phase
6. Counter electrode (organic phase)
7. Glass vessel
8. Reference electrode (organic phase)
9. Teflon body

with iR drop compensation was employed in the experiments.

For dc cyclic voltammetric measurements, a small triangular voltage, 25 mV s^{-1} ramp was generated using PM 1502 Electroanalyser. The current out put of the potentiostat was connected directly to a LLOYD PL3 X-Y/t recorder. For ac cyclic voltammetric measurements, a small amplitude (5.5 mV peak to peak) sinusoidal signal from a frequency generator (Tektronix AF 501) was superimposed on a 10 mV s^{-1} triangular sweep (continuous technique) or applied at a constant voltage (point by point technique). The current out put of the potentiostat was connected to a lock-in-analyzer (PAR Model 5204), which was used for the continuous measurements of the inphase and quadrature components of the ac current. The out put of the lock-in analyzer was connected to the X-Y recorder. The out put of the potentiostat was also connected to an ascilloscope (Tektronics Model 501) to regulate the proper compensation of the iR drop across the interface. The iR compensation was set to the nearest point before oscillation.

For a check of the frequency response of the potentiostat, both a series and parallel RC circuits were constructed from a dummy cell. The observed spectrum of the dummy cells is shown in Figures 4.3 and 4.4. It comes out to be a vertical line for the RC series circuit and a semi-circle for the parallel RC circuit as expected.

The inphase and quadrature components of the sinusoidal current flowing through the interface were

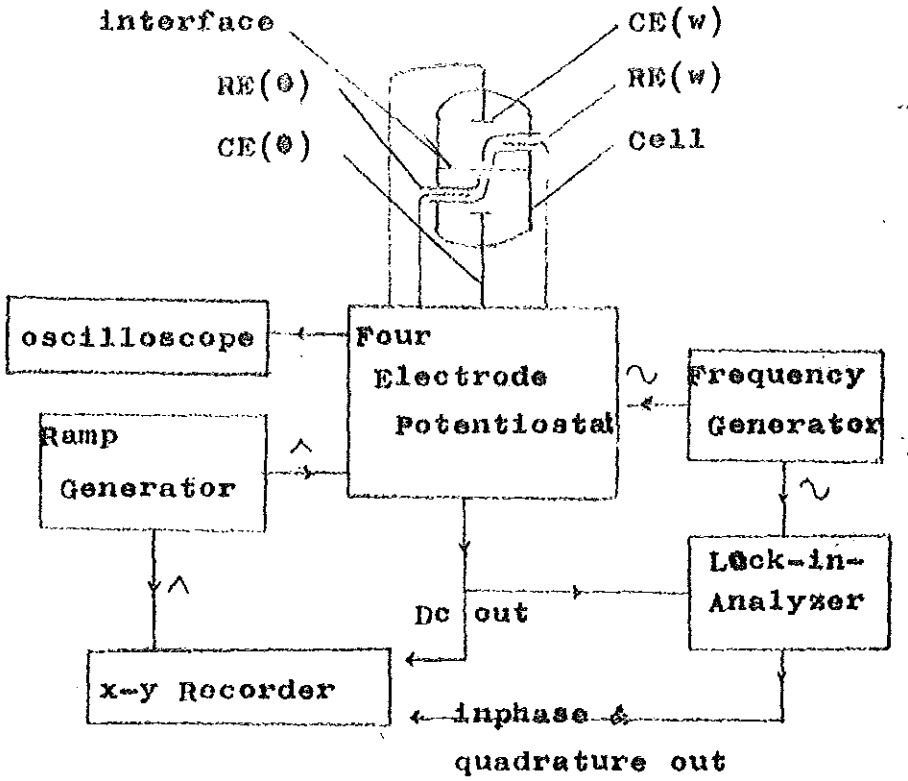

Figure 42. Block diagram of the electronic set up. CE(O) and CE(W) are couter electrodes in the organic and aqueous phases respectively, and RE(O,W) are reference electrodes of the organic and aqueous phases respectively.

read or measured at the out put of the lock-in-analyzer at frequencies between 20 Hz and 280 Hz. They were transformed into the real Z' and the immaginary Z" impedance components using the equations (3.7.2), (3.7.3), (3.7.7) and (3.7.8).

For a check of the reference electrodes in the experiments, hexafluorophosphate (PF_6^-) anion was used as an internal reference ion in situ, i.e. after the impedance measurements were complete, a drop of 10 mM NH_4PF_6 solution was dissolved in the aqueous phase and the ac cyclic voltammogram of PF_6^- ion transfer from water to o-DCB was measured.

For conductivity measurements, stock solution of 1 mM PNPDCC in water saturated o-DCB was prepared. The desired concentrations were prepared from the stock solution by successive dilution. Five different concentrations $1x10^{-4}$ mol/l to $5x10^{-4}$ mol/l were prepared and the conductivity of each solution was measured at 25°C using (PHILP HARRIS) conductivity meter. The cell constant was determined by measuring the conductivity of standard (0.74526 g/l) KCl solution, and was found to be 1.41.

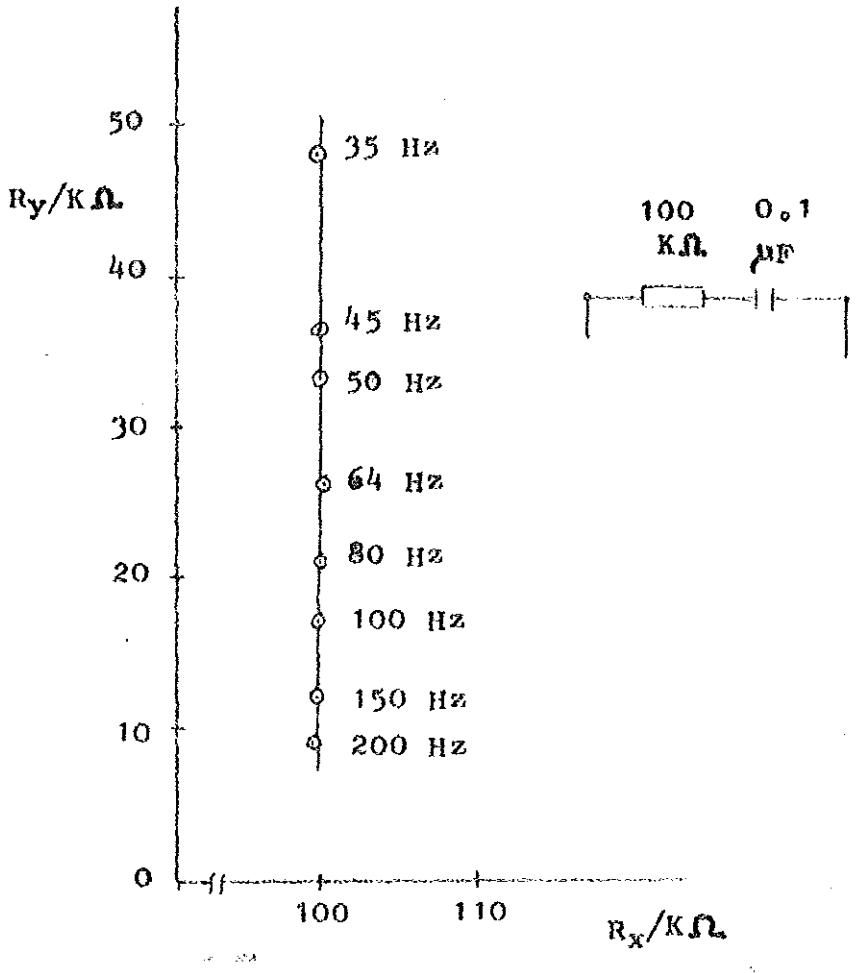

Figure 43. The response of the potentiostat for the series RC dummy cell shown for frequencies between 35 and 200 Hzs.

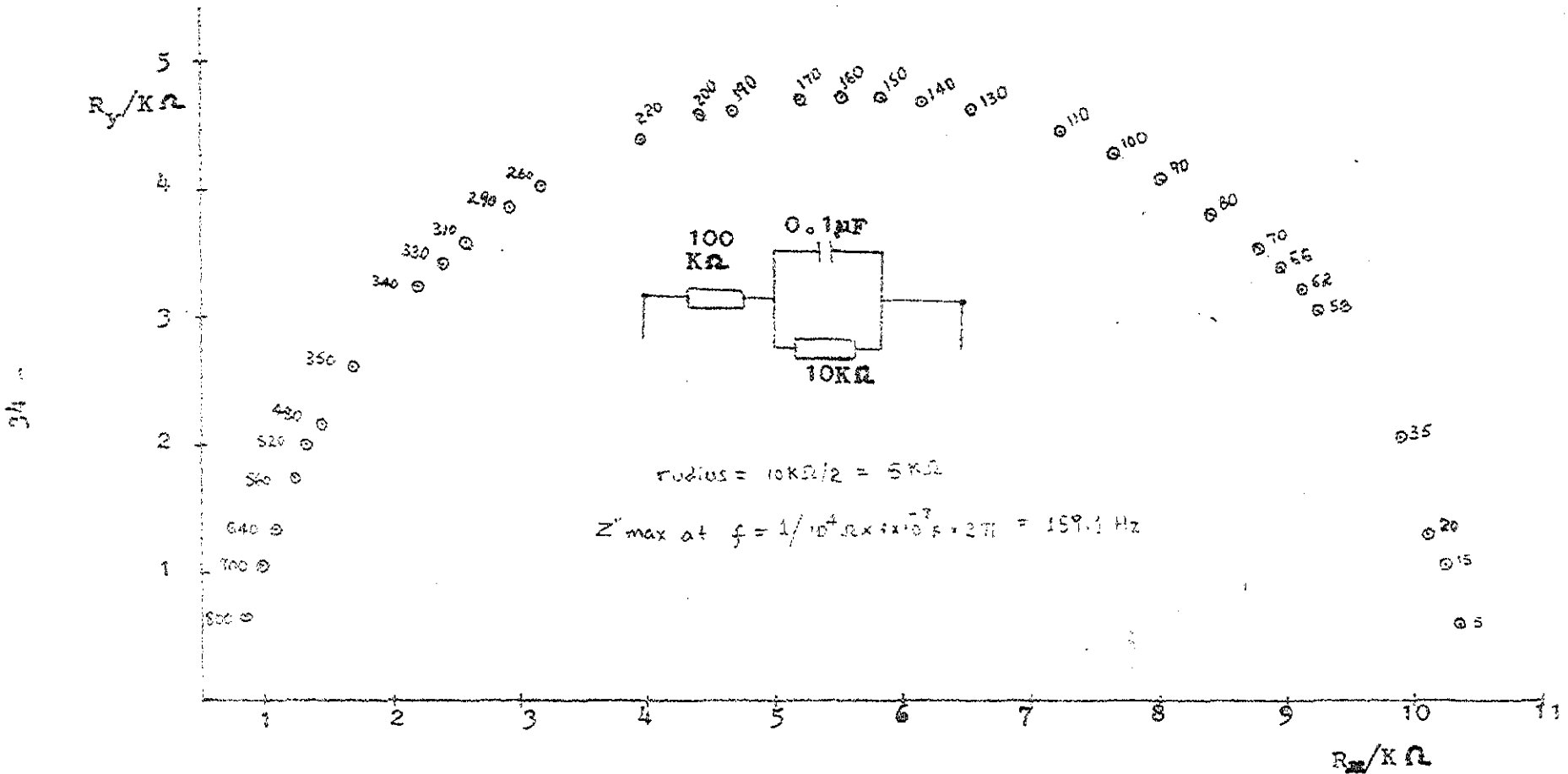

Figure 44 The response of the potentiostat for paraller RC dummy cell shown for frequencies between 5 and 800 Hzs.

5. RESULTS AND DISCUSSION

5.1. Fixing the Zero Point of the Potential Scale

The method employed to fix the potential scale in the systems water/nitrobenzene, water/1,-dichloroethane (90) and water/p-nitrophenyloctylether (33) by using TPAsTPB as supporting electrolyte in the organic phase could not be applied in o-DCB due to the low solubility of TPAsTPB in o-DCB. Therefore a 10 mM solution of PNPDCC saturated with TPAsTPB served as a base electrolyte in the organic phase to fix the zero point on the $\Delta^{w}_{o}\phi$-scale as shown in figure 5.1. It is clear from figure 5.1 that the transfer of TPB^- from o-DCB to water occurs about 40 mV more negative than the transfer of Li^+ from water to o-DCB. The transfer of the bulky hydrophobic DCC^- ion from o-DCB to water is not supposed to occur before the transfer of Li^+.

5.2. Influence of the Supporting Electrolytes on the Potential Window

Figure (5.2) and (5.3) show the influence of the supporting electrolytes in both the aqueous and organic phases. In both cases the transfer of Li^+ from water to o-DCB cuts off the potential window at positive potentials while at negative potentials the transfer of Cl^- ion from water to o-DCB is the limiting charge transfer reaction when LiCl is used as a supporting electrolyte in the aqueous phase (Figure 5.2 curve 2).

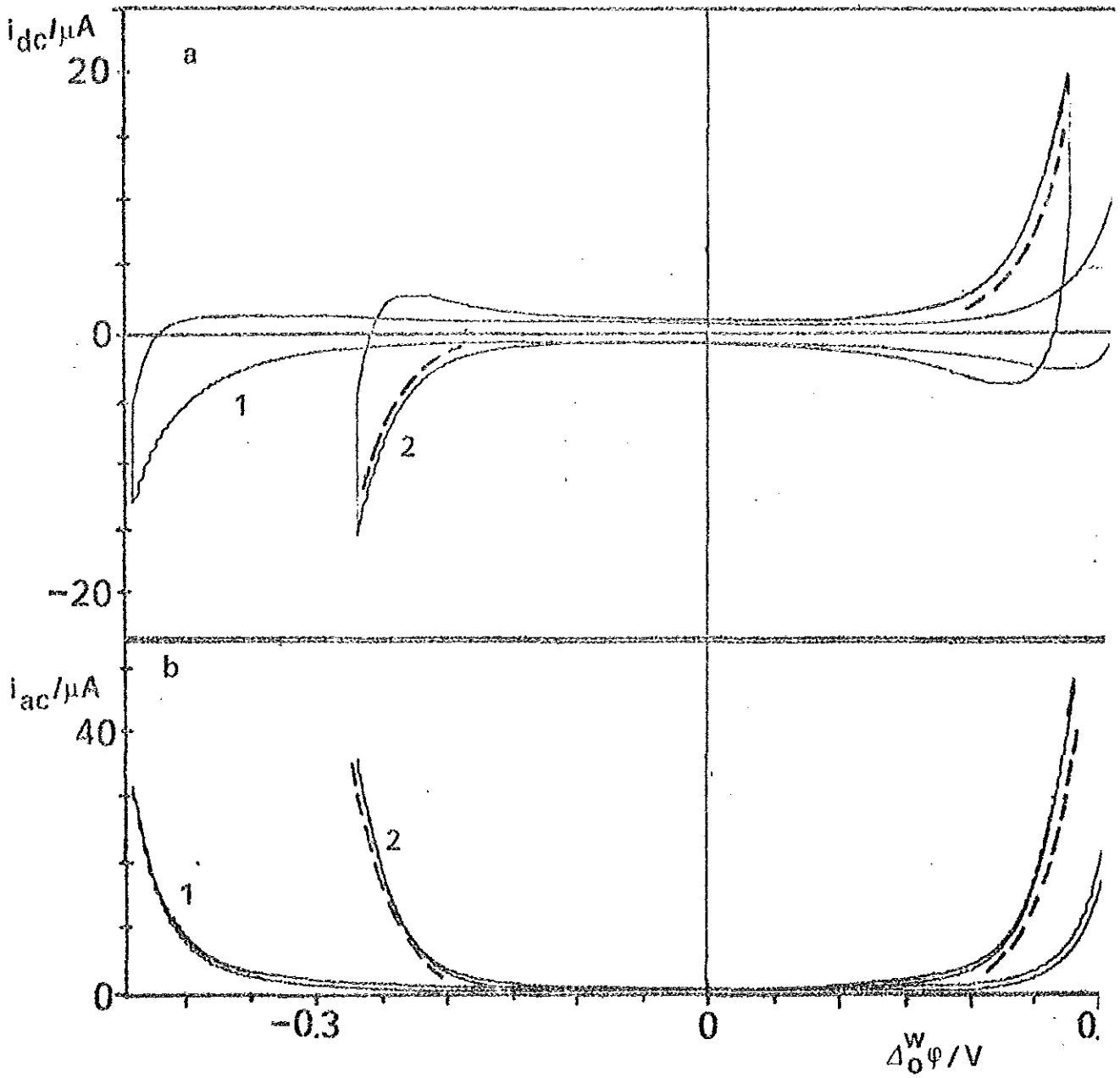

Figure 5.1 The dc(a) and ac(b) cyclic voltammograms of the water/o-DCB interface showing the determination of $\Delta\varphi=0$. Supporting electrolytes 5 mM Li_2SO_4(w) and 10 mM PNPDCC(o-DCB). Sweep rate a) 25 mVs^{-1}, b) 10 mVs^{-1}. (1) Supporting electrolyte only, (2) organic phase saturated with TPAsTPB, f=35 Hz.

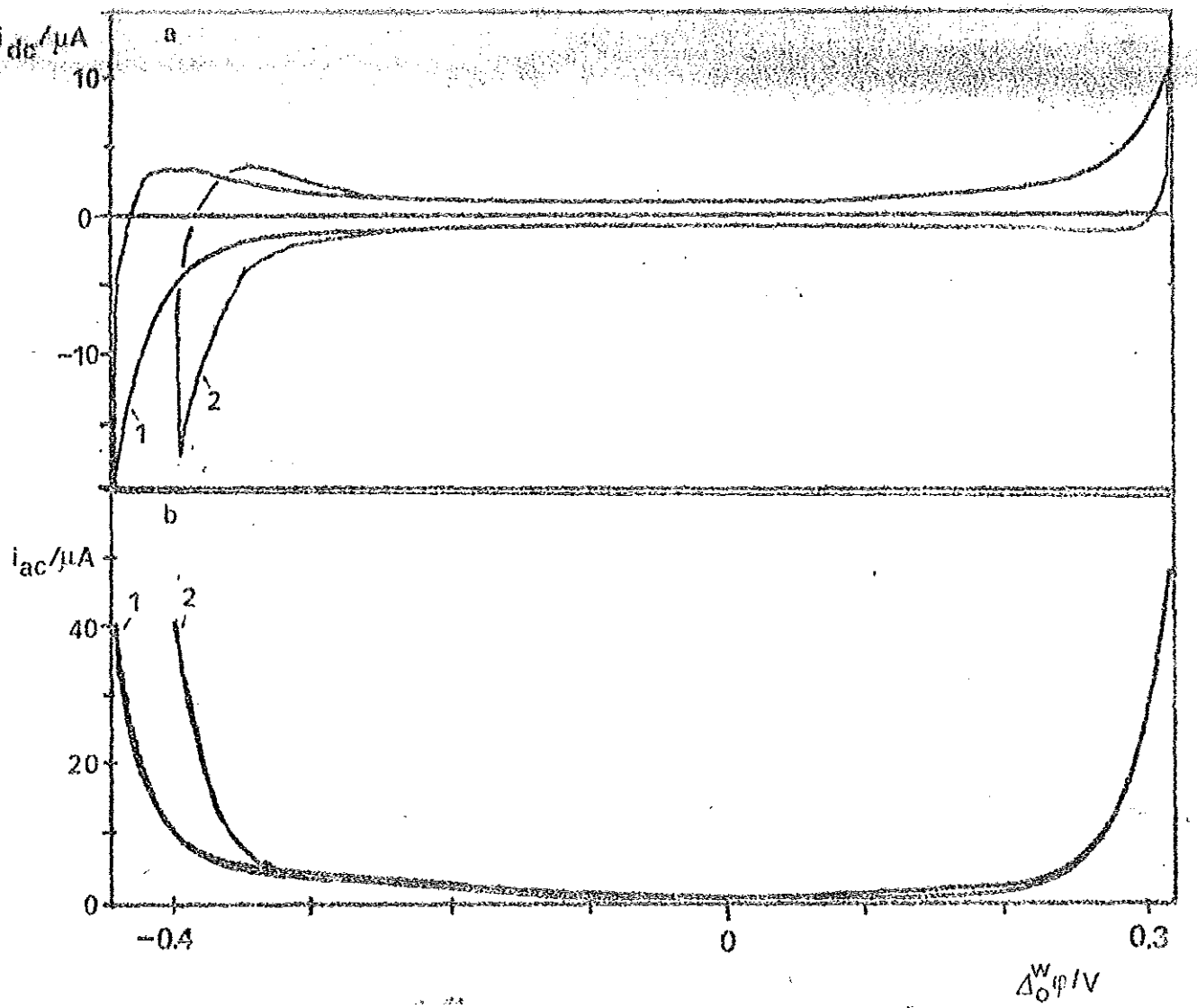

Figure 5.2 DC(a) and ac(b) cyclic voltammograms at water /o-DCB interface. Sweep rate a) 25 mV/s and b) 10 mV/s, f = 35 Hz. Supporting electrolyte 10 mM PNPDCC(o-DCB) and 1) 5 mM Li_2SO_4(w) and 2) 10 mM LiCl(w).

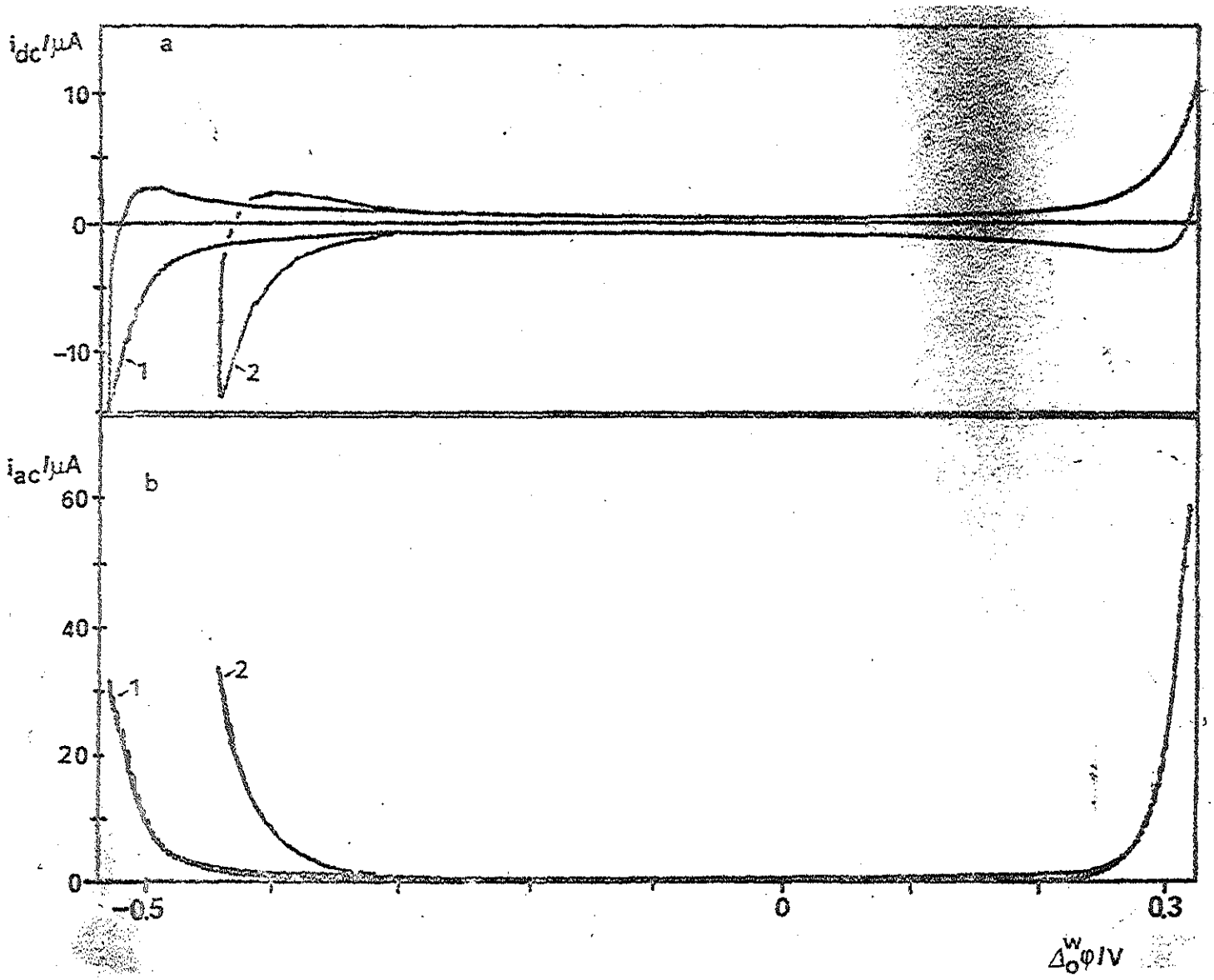

Figure 5.3 DC(a) and ac(b) cyclic voltammograms at the water/o-DCB interface. Supporting electrolyte 10 mM LiF(w) and 1) 10 mM TDADCC(o-DCB) 2) 10 mM PNPDCC(o-DCB). f = 20 Hz, Ea = 5.5 mV peak to peak, sweep rate 25 mV/s(a) and 10 mV/s(b).

The same voltammogram is obtained with PNPDCC in o-DCB independent of wether Li_2SO_4 (Figure 5.1 curve 1 and Figure 5.2 curve 1) or LiF (Figure 5.3 curve 2) is the supporting electrolyte in the aqueous phase. Curve 1 of Figure 5.2 can either be due to the transfer of PNP^+ from o-DCB to water or due to the transfer of SO_4^{-2} from water to o-DCB. When Li_2SO_4 is replaced by LiF as a base electrolyte in the aqueous phase, the same voltammogram is obtained (Figure 5.3 curve 2). Hence the assumption seems to be justified that PNP^+ is transfered from o-DCB to water before the transfer of SO_4^{-2} or F^- ions from water to o-DCB. On the other hand an extension of the potential window by about 100 mV can be achieved when PNP^+ is replaced by tetradodecylammonium (TDA^+) in the organic phase (Figure 5.3 curve 1). Neverthless, the potential window obtained by employing PNPDCC in the organic phase is wide enough for the studies of the transfer of even relatively hydrophilic ions like NO_3^- and ClO_4^- by dc or ac cyclic voltammetry.

5.3. Simple Ion Transfer

Figure 5.4 shows a typical ac cyclic voltammogram for the transfer of some ions from water to o-DCB, and from which the half-wave potentials of the ions studied can be obtained from the peak potentials. Figure 5.5 shows that the separation of the peak potentials on the dc cyclic voltammograms for the transfer of PF_6^- is about 60 mV, independent of the sweep rate upto 100 mV/s, while Figure 5.6 shows the dependency of the peak current

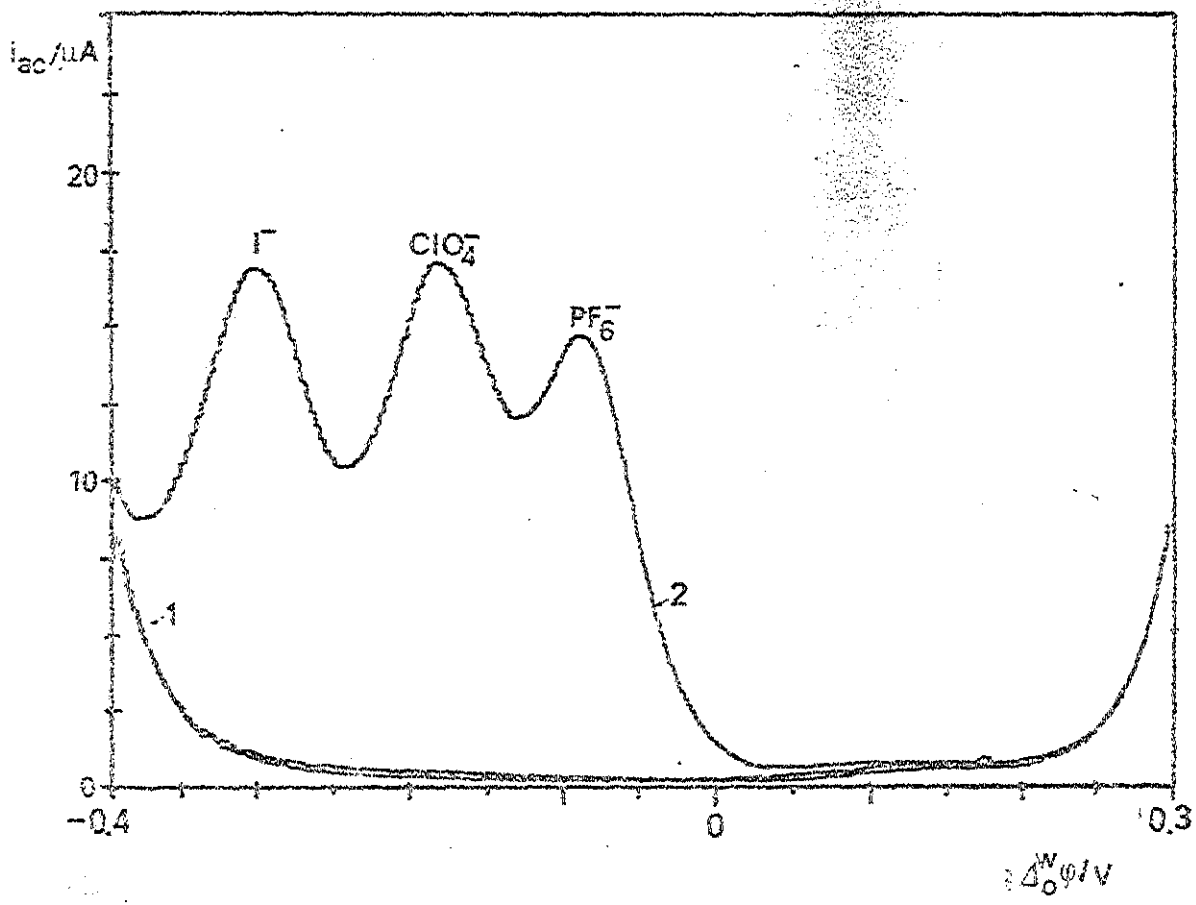

Figure 5.4 Ac cyclic voltammogram at water/o-DCB interface. Supporting electrolytes 5 mM Li_2SO_4(w) and 10 mM PNPDCC(o-DCB). (1) Only supporting electrolytes. (2) After addition of 0.1 mM of NH_4PF_6, $LiClO_4$ and NaI. f = 35 Hz, sweep rate 10 mV/s.

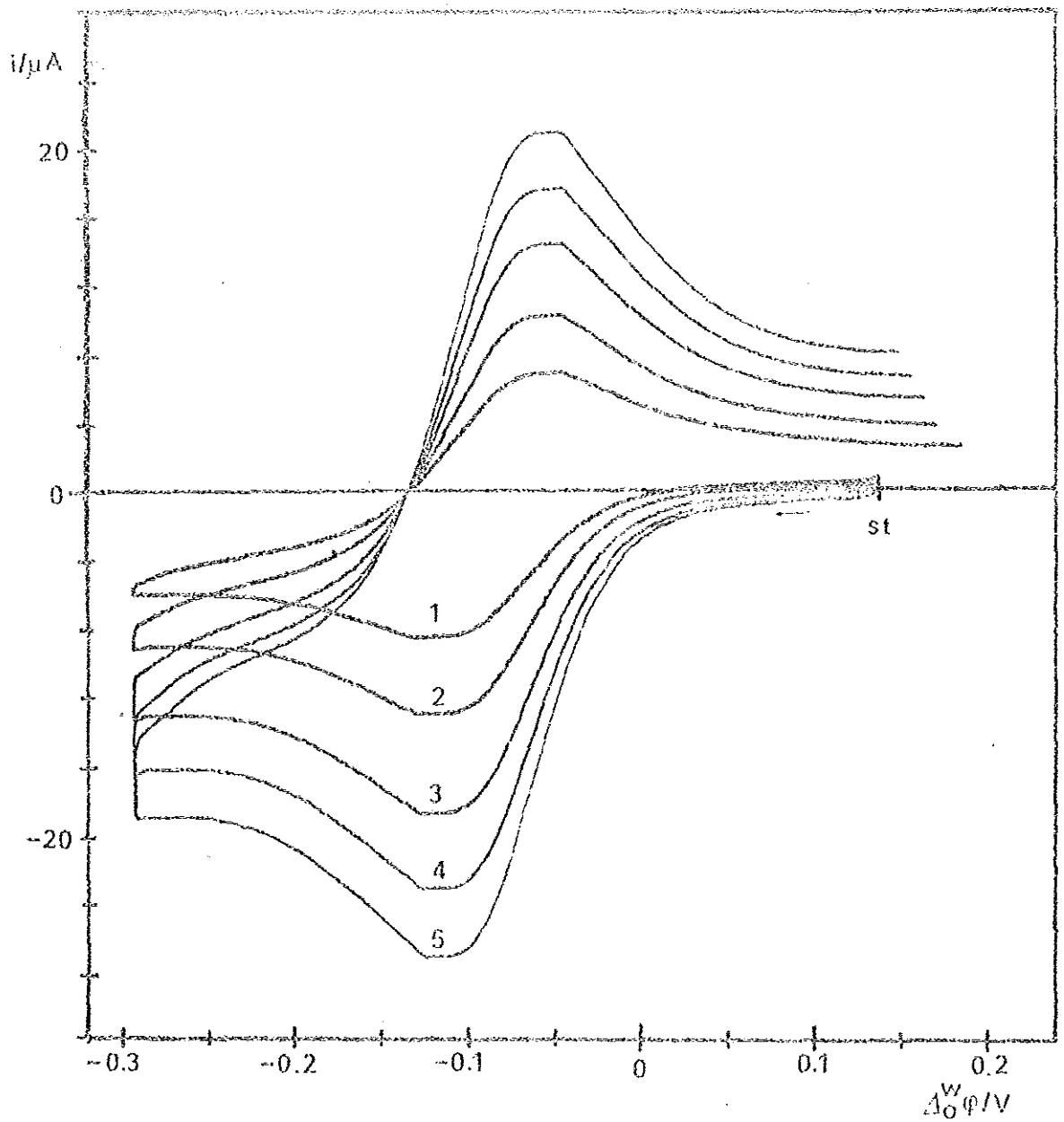

Figure 5.3 DC cyclic voltammograms at the water/O-DCB interface. Aqueous phase Li_2SO_4 10^{-4} mol/l NH_4PF_6. Sweep rate 10(1); 25(2); 50(3); 75(4); and 100(5) mV/s.

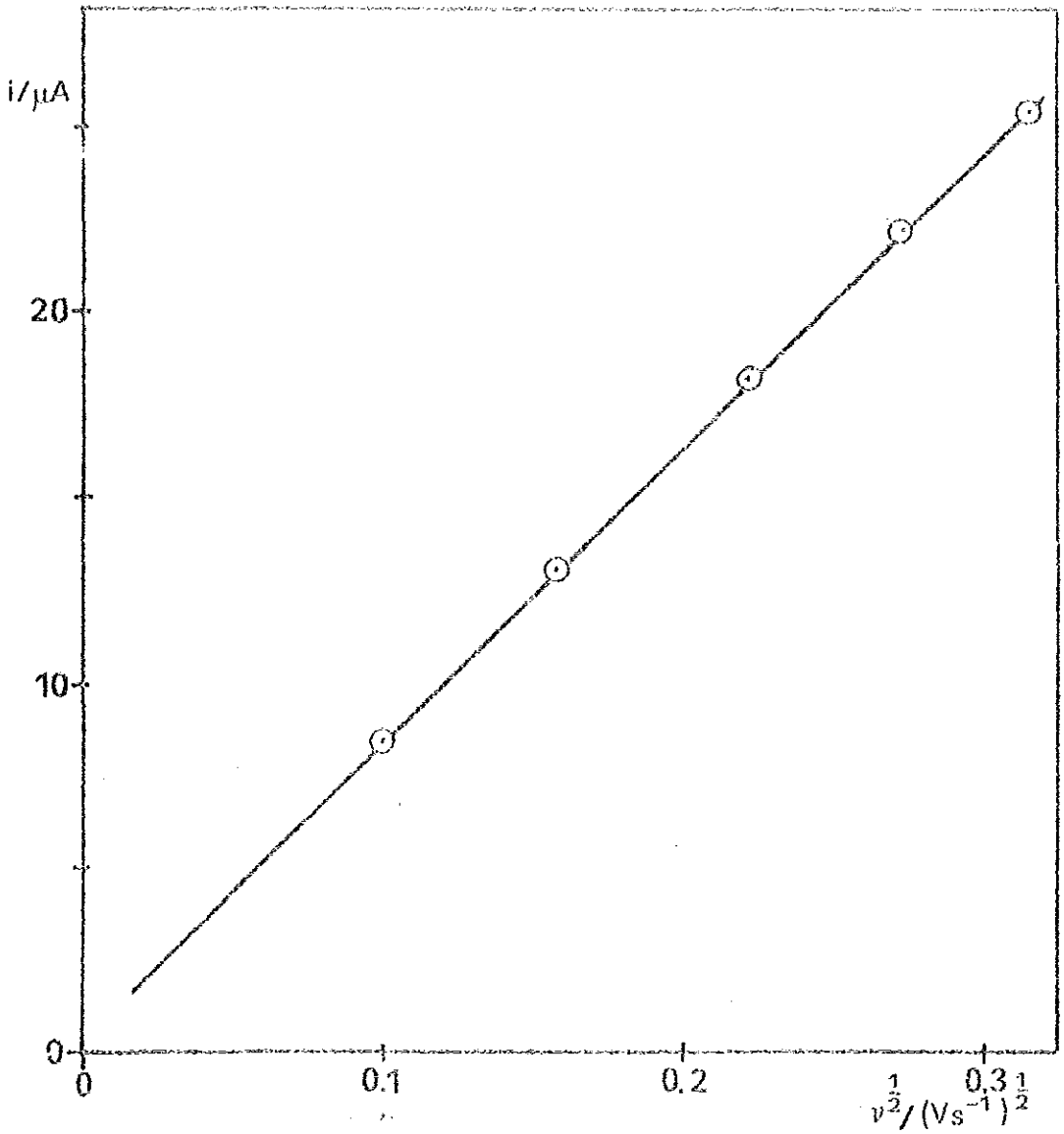

Figure 5.6 Dependence of peak current for the transfer of PF_6^- ion from water to o-DCB on the sweep rate. Conditions as in Fig. 5.5.

on $v^{\frac{1}{2}}$, indicating that the ion transfer across the water/o-DCB interface is diffusion controlled at low sweep rates. Furthermore, the half-peak width of the ac voltammogram is 90 mV and the forward and the reverse scans coincide at low ac frequencies. This can be taken as a further criterion for the diffusion control of the ion transfer. The diffusion coefficient of PF_6^- in water was obtained from the slope of Figure 5.6 and found to be 1.4×10^{-5} $cm^2 s^{-1}$. This value agrees fairly well with the diffusion coefficient of PF_6^- ($D_\infty = 1.57 \times 10^{-5}$ $cm^2 s^{-1}$) calculated from the equivalent conductance at infinite dilution given in Ref. (85).

The half-peak Galvani potential difference of the ions studied are compiled in Table 5.1. The evaluation of the standard Galvani potential difference $\Delta_o^w \varphi^o$, and the standard Gibbs energy of transfer $\Delta G_t^{o,\alpha \to \beta}$, is not as straight-forward as in the system water/nitrobenzene, where ion association in nitrobenzene may be neglected, but must be taken into account in o-DCB. The standard Galvani potential difference of an ion can be evaluated from the experimental half-wave potential by the rearrangement of equation (3.1.9)

$$\Delta_o^w \varphi^o = \Delta_o^w \varphi_{\frac{1}{2}} + \frac{RT}{zF} \ln \left\{ 1 + K_A C_o \alpha \gamma_\pm^2(o) \left[\frac{D_A(w)}{D_i(o)} \right]^{\frac{1}{2}} \right\} - \frac{RT}{zF} \ln \frac{\gamma_\pm(o) \left[D_+(w) \right]^{\frac{1}{2}}}{\gamma_\pm(w) \left[\quad \right]} \qquad (5.3.1)$$

where C_o and α are the analytical concentration and the degree of dissociation of the supporting electrolyte in

Table 5: Half-wave potentials and Derived Thermodynamic Quantities

Ion	r_i/nm[c]	$D(w)\times10^{5}$ $cm^2\ s^{-1}$	$D(o)\times10^{6}$ $cm^2\ s^{-1}$	$K_A\times10^{-6}$	$\Delta\varphi_{1/2}$	$\Delta\varphi^{o}/V$	ΔG^{o}_{p} $kJmol^{-1}$	ΔG^{o}_{t}cal[d] $kJmol^{-1}$
TPA^+[a]	0.425	0.526	3.8	0.4	-0.316	-0.273	-26.3	-
TAA^+[a]	0.443	0.462	3.8	0.37	-0.323	-0.283	-27.3	-28
TEA^+	0.413	0.513	4.3	0.42	-0.177	-0.131	-12.6	-15
TPA^+	0.379	0.616	4.9	0.49	-0.080	-0.032	-3.1	-1
TEA^+	0.337	0.853	6.2	0.61	0.067	0.116	11.2	13
THA^+	0.280	1.18	6.7	0.86	0.226	0.277	26.73	26.0
I^-	0.220	2.04	6.11	6.4	-0.319	-0.406	39.2	-
ClO_4^-	0.240	1.79	7.00	5.1	-0.182	-0.266	25.7	-
MnO_4^-	0.250	1.63	6.5[b]	4.5	-0.129	-0.208	20.1	-
BF_4^-	0.228	-A	-A	5.8	-0.248	-0.332	32.0	-
PF_6^-	0.260[c]	1.57	5.0[b]	4.1	-0.088	-0.165	15.9	-
$PtCl^-$	-	0.815	4.58	4[b]	-0.049	-0.135	13.0	-
SCN^-	-	1.76	6.0[b]	-	-0.285	-	37.2	-
NO_3^-	0.179	1.90	7.17	11.0	-0.389	-0.489	47.2	-
ClO_3^-	0.200	1.72	6.04	8.3	-0.375	-0.468	45.2	-
TPB^-	0.420	0.526	4.0	0.36	+0.316	+0.273	-26.3	-

A) The correction due to the diffusion coefficient was based on the average value of the other anions(¼ π).

B) Estimated values, C) Taken from Ref.(79). D) B. Hundhammer unpublished result.

the organic phase respectively, K_A is the association constant of the associate formed between the ion investigated and the respective counter ion of the supporting electrolyte. D_A is the diffusion coefficient of the associate in the organic phase. All other symbols have their usual meanings. The association constant of PNPDCC in water saturated o-DCB was determined from the conductivity data shown in Table 5.2 by the Shedlevsky method (83) using equations from (3.5.5) to (3.5.9). The Λ_o value for equation (3.5.7) was first approximated from the plot of $1/\Lambda$ vs $C\Lambda$ of equation (3.5.4), the intercept of which gives $1/\Lambda_o$. From the slope of the plot of $1/\Lambda s(z)$ vs $C\Lambda\gamma_{\pm}^2 s(z)$ the association constant of PNPDCC in o-DCB was found to be 2×10^3 (on the molar scale). The mean activity coefficient, and the degree of dissociation in the organic phase can then be obtained by interation from the Debye-Huckel equation

$$\log\gamma_{\pm}\,(o) = \frac{-A(C_o\alpha)^{\frac{1}{2}}}{1+Ba(C_o\alpha)^{\frac{1}{2}}} \qquad (5.3.2)$$

and the respective expression for the association constant:

$$K_A = (1-\alpha)/\alpha^2 C_o \gamma_{\pm}^2 \qquad (3.5.2)$$

where A and B are parameters of the Debye-Huckel theory which depend on the dielectric constant of the solvent and temperature. The values of A and B were found to be 11.04 $mol^{-\frac{1}{2}}$ $dm^{3/2}$ and 9.24×10^7 $cm^{-1}mol^{-\frac{1}{2}}$ $dm^{3/2}$ respectively. a is the ion size parameter and was set equal to the sum of the ionic radii of PNP^+ (r = 0.46 nm)

Table 5.2. Conductivity data used for the evaluation of K_A for PNPDCC in o-DCB.

C(PNPDCC) mol/l	/Sm^{2}eq^{-1}
1×10^{-4}	21.86
2×10^{-4}	22.56
3×10^{-4}	23.80
4×10^{-4}	25.24
C→0	28.18

Λ_0= 28.18 and $K_A = 2.00\times10^3$

a = 10.4 nm was taken a distance parameter in Debye-Huckel equation.

Table 5.3. Association constants for some electrolytes in 1,2-dichloroethane and o-DCB.

Electorlyte	$K_A \times 10^{-4}$	
	1,2-DCE	o-DCB
TMAPic	3.12[a]	-
TEAPic	0.63[a]	8.76[d]
TPAPic	0.52[a]	7.64[d]
TBAPic	0.433[b]	5.85[b]
	0.436[c]	5.72[d]
TAmPic	0.42[a]	5.50[d]
TBATPB	0.171[b]	1.03[b]
$TBAClO_4$	0.641[c]	9.33[b]
		9.6[c]
$TBANO_3$	0.820[b]	20[b]
PNPDCC	-	0.2[e]

a) Taken from Ref.(80), b) Ref.(81), c) Ref. (82) d) Ref (83), and e) this work.

and DCC^- (r = 0.58 nm). Using equations (5.3.2) and (3.5.2) the degree of dissociation x, and the mean activity coefficient $\gamma_\pm$ of PNPDCC in o-DCB were found to be 0.46 and 0.35 respectively. An activity coefficient of 0.88 has been used for all monovalent ions in the aqueous phase (5 mM Li_2SO_4). The ratio $D_A(o)/D_i(o)$ was approximated by $r_i/(r_i+r_c)$, r_i and r_c being the radius of the ion studied and the counter ion respectively. The diffusion coefficients used in the calculation are included in Table 5.1. The diffusion coefficients in the aqueous phase are based on limiting equivalent conductances, Λ_o given in Ref. (85). Since only a few values (ClO_4^- , NO_3^- , I^-, Pic^-) have been reported in o-DCB (86) the diffusion coefficient of tetraalkylammonium, $TPAs^+$ and TPB^- are based on the average Walden product of the respective ion given in Ref. (86). The standard Gibbs energy of partition $\Delta G_p^{o,w\rightarrow o\text{-DCB}}$, was obtained from the standard Galvani potential difference $\Delta_o^w\phi^o$, using equation (3.1.5). The estimation of the association constant K_A, of the ion with the counter ion of the supporting electrolyte can be obtained from the Fuoss approach (88). Using the sum of ionic radii of the ions as a distance parameter a (contact pair), the association constants calculated for the ions are given in Table 5.1. The estimation of K_A is a crucial point in obtaining a reliable set of standard Galvani potential differences. Association constants reported for several electrolytes in o-DCB are compiled in

Table 5.3. Comparison of association constants of the electrolytes in o-DCB and in nearly isodielectric solvent 1,2-dichloroethane shows that the association constants in o-DCB are found to be more than 10 times that of 1,2-DCE. This experimental fact has been explained by Gilkerson (87) by taking into account specific ion-solvent and ion-pair-solvent interactions.

In order to check the results of the values of the standard Galvani potential difference and the standard Gibbs energies of partition by an independent method, $\Delta G_p^{o,w\to o\text{-DCB}}$, of the salts TPAsTPB, TPPTPB and TBATPB were dtermined from the solubility of these salts in wet o-DCB at 25°C. The solubilities obtained from the average of a triplicate determination were 4.24×10^{-4} mol l^{-1}, 5.14×10^{-4} mol l^{-1} and 4.55×10^{-3} mol l^{-1} for TPAsTPB, TPPTPB and TBATPB respectively. The thermodynamic data together with the constants used in eval evaluation of x and y by equations (5.3.2) and (3.5.2) are given in Table 5.4. The standard Gibbs energy of partition of either TPAsTPB or TPPTPB may be split into single ion values (89) from which in turn the standard Galvani potential difference for ions $TPAs^+$, TPP^+ and TPB^- can be obtained. The average $\Delta G_p^{o,w\to o\text{-DCB}}(TPAs^+) = \Delta G_p^{o}(TPP^+) = \Delta G_p^{o}(TPB^-) = -27.8$ KJ mol^{-1} is in good agreement with the value of -27.7 KJ mol^{-1} calculated from Kim's result (91) as well as with the value obtained by voltammetric determination. $\Delta G_p^{o}(TBA^+)$ is obtained from $\Delta G_p^{o}(TBATPB)$ and $\Delta G_p^{o}(TPB^-)$ using equation (3.4.7).

Table 54. Thermodynamic data obtained from the solubility data of the respective salts in water saturated o-DCB (25°C, molar scale)

salt	$K_A \times 10^{-4}$	a/nm	solubility 10^4 mol l^{-1}	pK_{sp}	ΔG°_t / kJ mol^{-1}	$\Delta G^{\circ}_t(H_2O)$ / kJ mol^{-1}	ΔG°_t(w)o-DCB) / kJ mol^{-1}
TPATPB	0.9	0.85	4.24	7.63	43.5	99.7[b]	-56.2
TPPTPB	0.9	0.85	5.14	7.53	42.9	97.7[c]	-54.8
TBATPB	1.03[a]	0.83	45.50	6.48	36.92	75.1[c]	-38.2

a) Taken from Ref.(31), b) Ref(34), c) Ref.(47).

$\Delta G_p^o(TBA^+) = \Delta G_p^o(TBATBP) - \frac{1}{2}\Delta G_p^o(TPAsTPB)$ and was found to be -10.4 KJ mol^{-1} which agrees fairly well w with the value of -12.6 KJ mol^{-1} obtained from voltammetric experiments. The standard Gibbs transfer energies calculated on the bases of the simple model of Abraham and Liszi (75) for some ions are listed in column 9 of Table 5.1. The observed good agreement of the calculated values which are obtained by the assumption that the non-hydrated ion exists with the organic phase underlines the capability of this simple model to obtain estimates of the Gibbs transfer energies.

Figure 5.7 shows the plot of G_p^o(o-DCB) vs G_p^o (1.2-DCE) from which a very good correlation (0.997) with a slope very close to unity.

5.4. Electrical Double Layer Studies

Figure 4.4 shows the response of the potentiostat for a simple RC parallel circuit which was used to test the frequency response of the potentiostat and also to check the method of measurements adopted in the studies. The values of the resistance and the capacitance were fairly accurately determined from the impedance plot. Thus the radius of the semicircle is Rct/2, and the maximum Z'' occur at $w = (RctC)^{-1}$, where Rct is the charge transfer resistance and C is the capacitance.

Figure 5.8 shows the range of potentials within which the current is controlled mainly by charging of

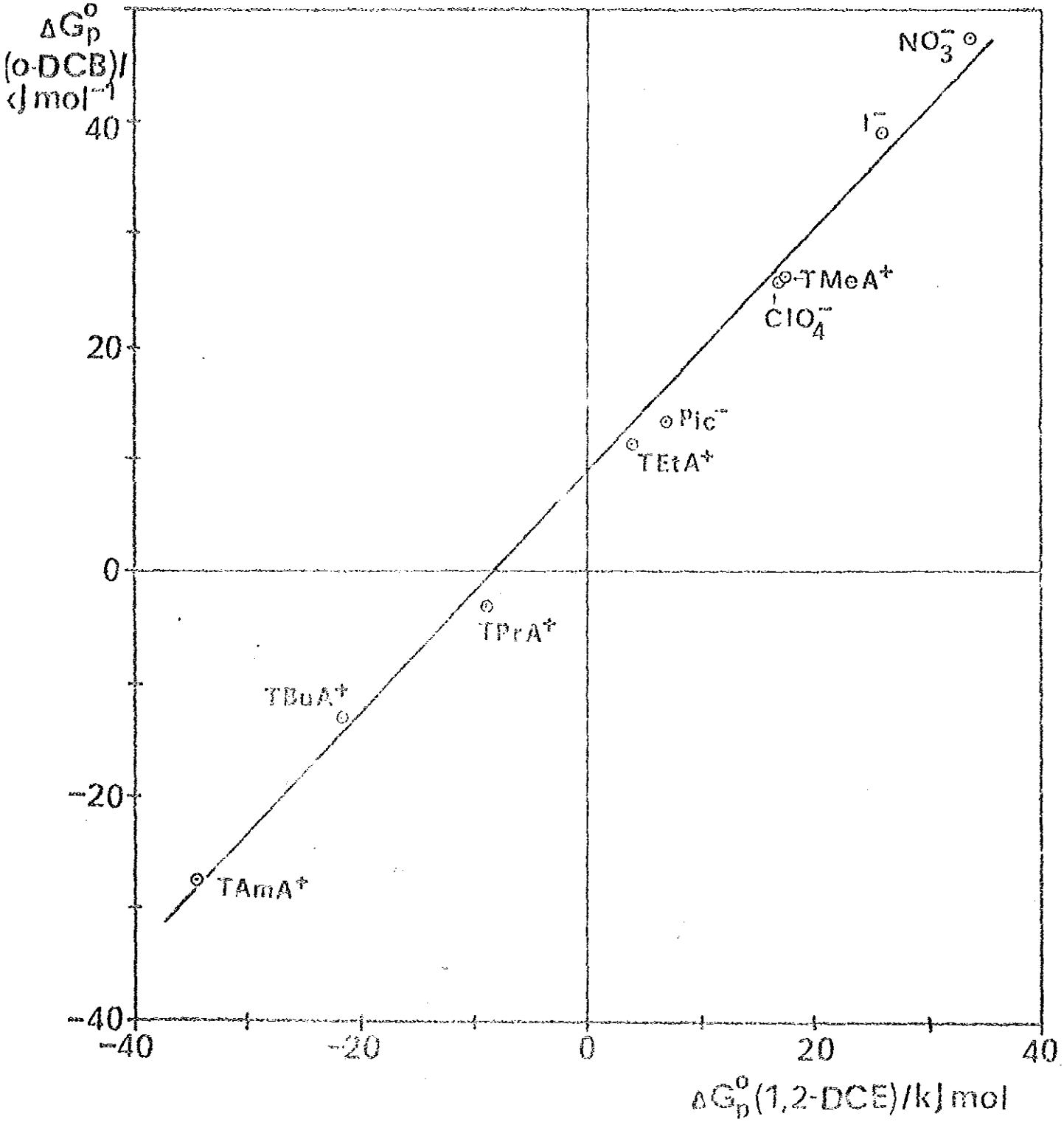

Figure 5.7 Plot of ΔG_p^o (o-DCB) vs $\Delta G^o{}_p$(1,2-DCE). Slope = 1,075, Intercept, 0.8 kJ, r=0.997.

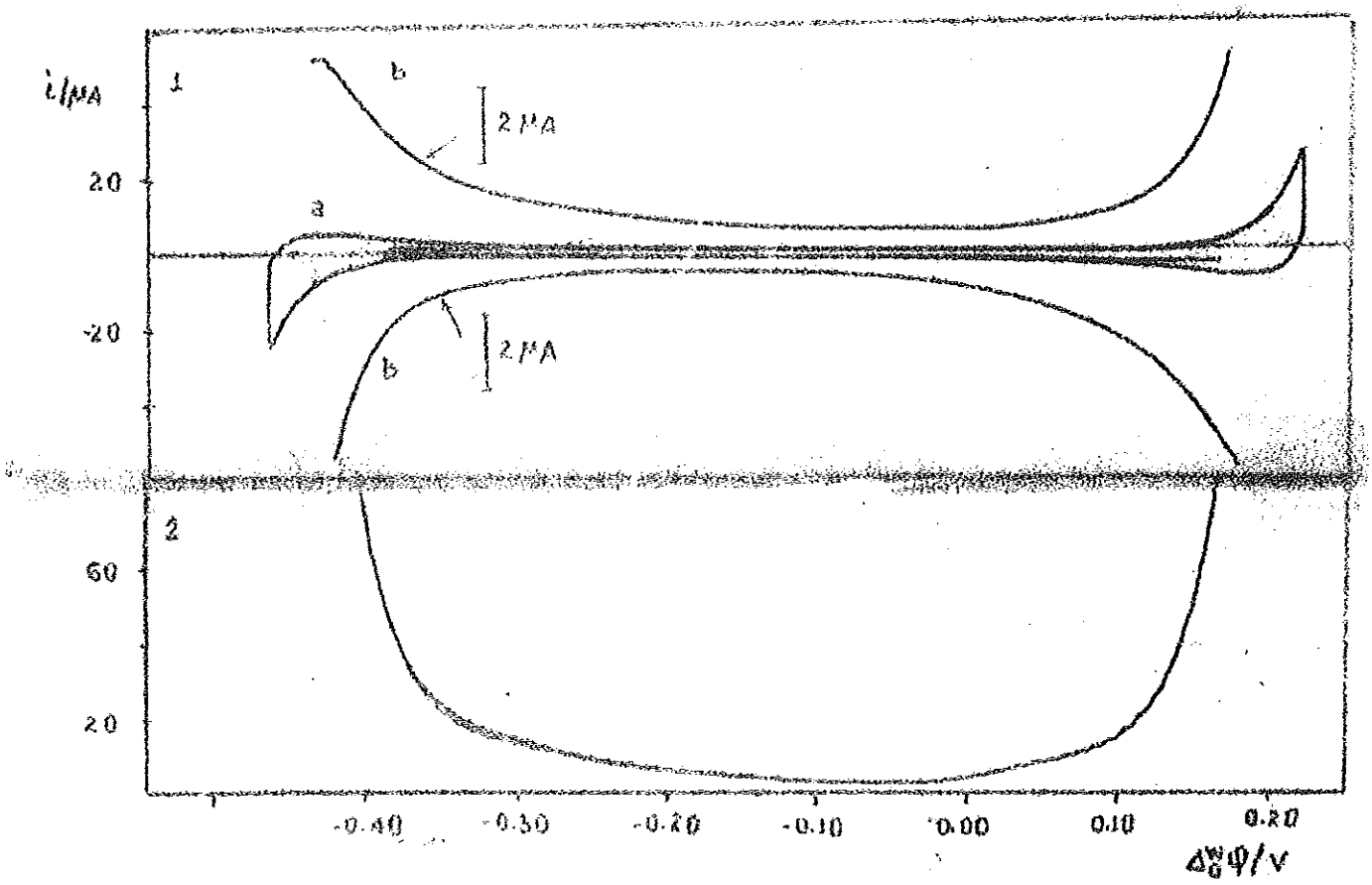

Figrue 5.8 dc(1) and ac (2) cyclic votammograms for the interface between 10 mM LiCl (W) and 10mM PNPDCC (o-DCB). Sweep rate 25 mV/s (1) and 10 mM/s (2), f=35 Hz (2).

the interface. In the potential range -0.40 V to +0.15 V the current corresponds mainly to the double layer charging and the system has the property required, while at more positive or more nggative potentials, the transfer of ions of the base electrolytes prevails. All impedance measurements were carried out within a potential range where charge transfer can be neglected. Figure 5.9 shows the ac voltammograms of the inphase and quadrature components at a frequency of 35 Hz of the system: 10 mM solution of LiCl in water and 10 mM solution of PNPDCC in o-DCB. The inphase and quadrature components of the ac current flowing through the interface were recorded as a function of potential at a given frequency between 35 and 130 Hzs. They were transformed into complex i impedance Z and phase angle δ using equations (3.7.8) and (3.7.7) respectively. The real Z', and imaginary Z", parts of the complex impedance can be obtained using equations (3.7.2) and (3.7.3).

Typical impedance plots are shown in Figure 5.10. These plots were resolved for electrical equivalent circuit of scheme (3.7.1). The small [illegible]

Figure 5.11 shows the plot of imaginary impedance Z" vs w^{-1} from the slope of which the capacitance of the double layer was obtained. Figure 5.12 shows the plot of interfacial capacitance as a function of potential at three different electrolyte concentrations in the aqueous phase. Assuming that the inner potential difference $\Delta_o^w\varphi_i$ = constant = 0, and taking into account

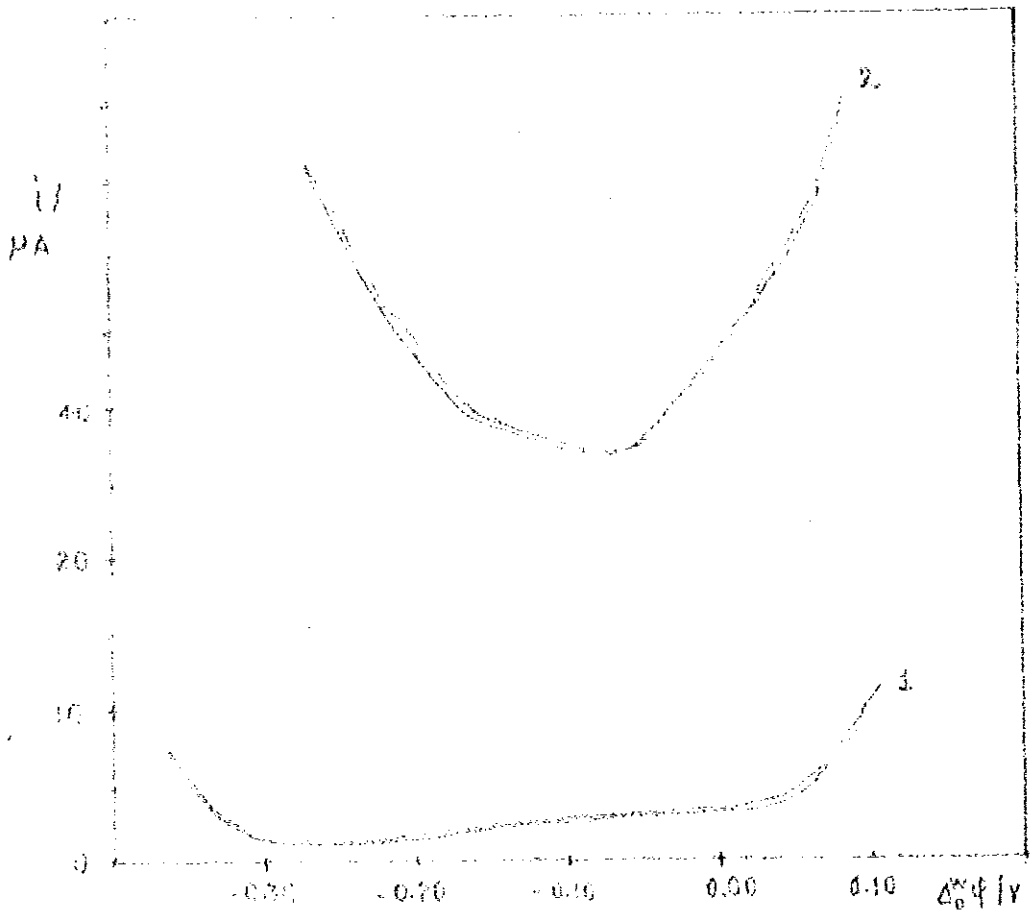

Figure 5.9 Inphase (1) and quadrature (2) components of ac impedance measurements for the interface between 10 mM LiCl (w) and 10 mM PBPDCC (o-DCB). Sweep rate 10 mV/s, f= 35 Hz.

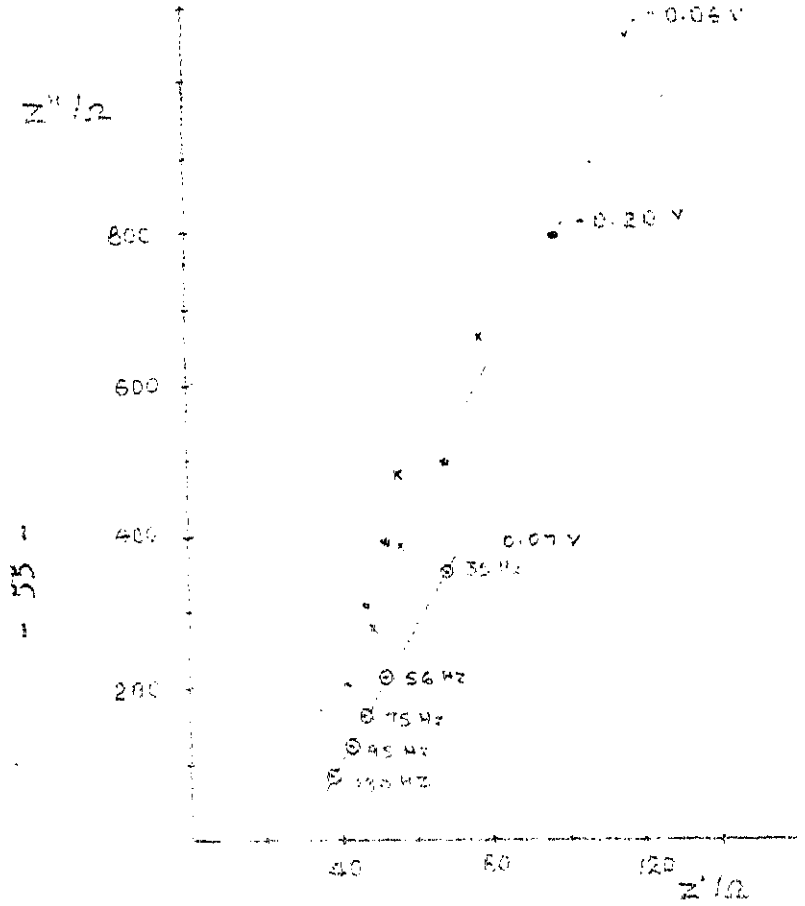

Figure 5.10 Impedance plot of the system 10 mM LiCl (w) 10 mM PNPDCC (o-DCB) at three different potentials and frequencies in Hz.

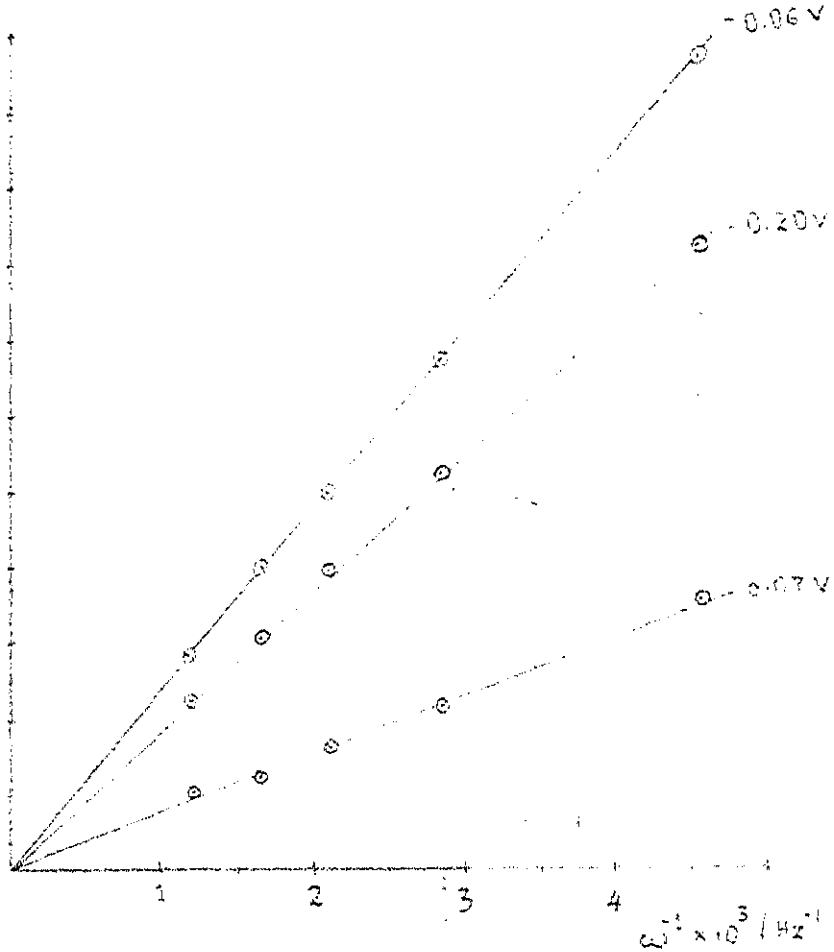

Figure 5.11 plot of Z_c vs w^{-1} for the same system.

ion-association in the organic phase, the diffuse layer capacitance C_d, was calculated by the Gouy-Chapman theory as discussed in Chapter Two. The values are given in Table 5.5. The dashed lines in Figure 5.12 are the plots of these theoretical diffuse layer capacitance as a function of potential.

From the experimental capacitance values the direct relationship between electrolyte concentration and interfacial capacitance is observed. Unlike the water/nitrobenzene (51) and water/1,2-dichloroethane (67) systems, the capacitance minimum which corresponds to the potential of zero charge occur at more negative potentials (-0.13 to - 0.12 V). This experimental fact can not be accounted from the present preliminary work only. Table 5.6 shows comparison of the theoretical and experimental capacitance minima for three different electrolyte concentrations. Comparison of the experimental capacitance with the theoretical capacitance i indicated that the theoretical capacitance calculated by the Gouy-Chapman theory is in good agreement from a qualitative point of view, but the quantitative agreement is not satisfactory.

Table 5.5. Theoretical diffuse layer capacitance at the interface between 0^{0} mM LiCl (w) and 10 mM PMTAC (o-PMTAC) calculated using the G-C theory.

$\Delta^{w}_{o}\varphi$ / V	Capacitance C_d / μF cm^{-2}		
	100 mM LiCl	10 mM LiCl	1mM LiCl
-0.30	94.15	52.35	29.34
-0.20	37.64	20.40	11.28
-0.10	13.25	8.43	4.77
-0.05	7.10	5.51	3.52
-0.03	5.82	4.83	3.26
-0.02	5.43	4.61	3.18
-0.01	5.19	4.48	3.14
0.00	5.11	4.43	3.12
0.01	5.19	4.48	3.14
0.02	5.43	4.61	3.18
0.03	5.82	4.83	3.26
0.05	7.10	5.51	3.52
0.10	13.25	8.43	4.77
0.20	37.64	20.40	11.28
0.30	94.15	52.35	29.34

Table 5.6. Capacitance minimum of theoretical and experimental values

Concentration of LiCl	100 mM	10mM	1 mM
Theoretical C_d μF/cm^{-2}	5.11	4.43	3.12
Experimental C/μF/cm^{2}	5.17	5.00	4.20

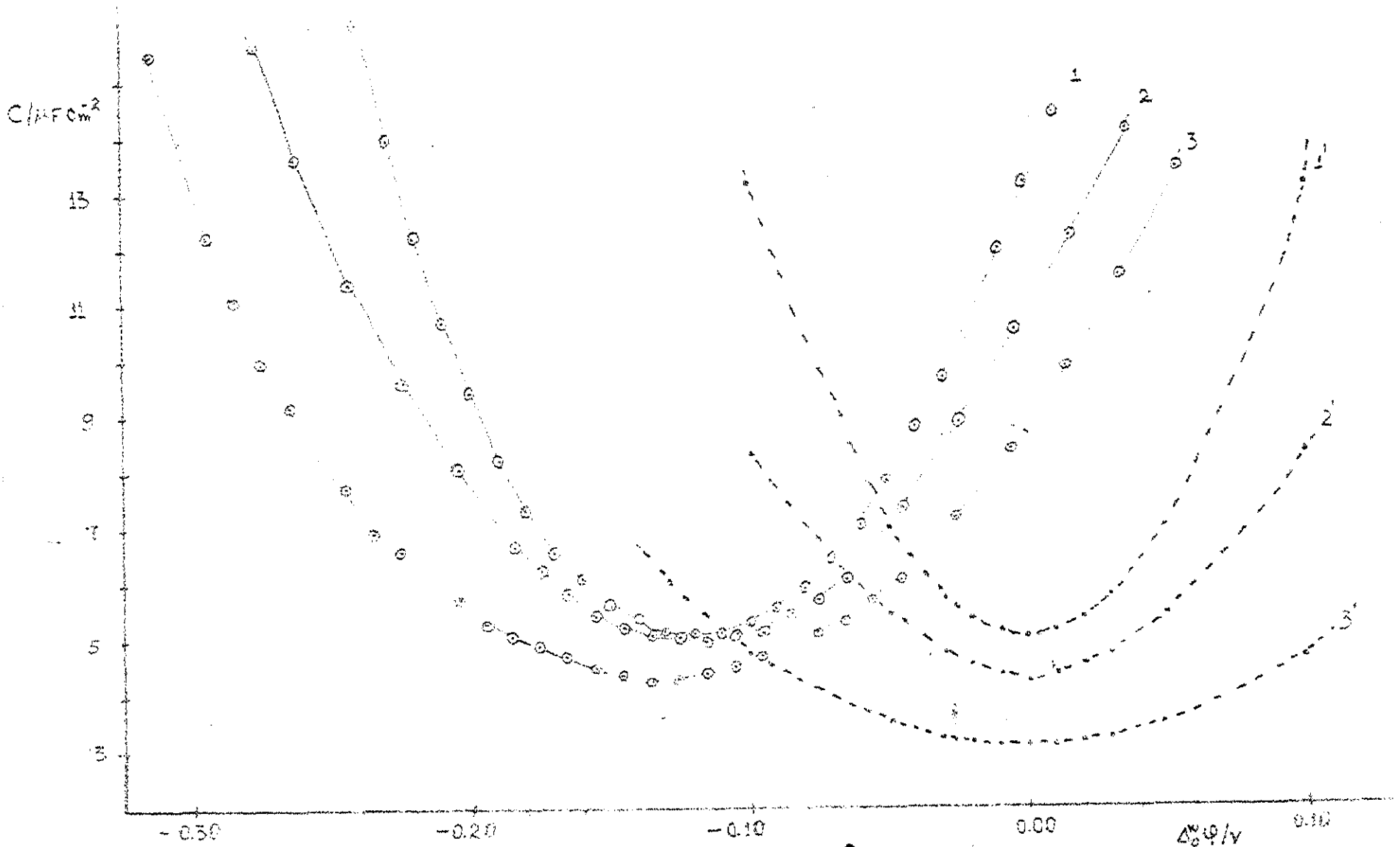

Figure 5.12 plots of interfacial capacitance C, vs $\Delta_o^w\phi$ for water/o-DCB interface containing 10 mM PNPDCC (o) and 100 mM LiCl(1,1') 10 mM LiCl(2,2') and 1 mM LiCl(3,3') in the aqueous phase. The dashed lines show the capacitance of the diffuse layer calculated using the Gouy-Chapman theory.

6. CONCLUSION

The zero point on the Galvani potential difference of the system water/o-DCB can be fixed by using a 10 mM solution of PNPDCC saturated with TPAsTPB as a supporting electrolyte in o-DCB. The potential window obtained by employing PNPDCC in o-DCB has been found to be wide enough for the studies of the transfer of even relatively hydrophilic ions like NO_3^- and ClO_4^- by ac and dc cyclic voltammetry. Furthermore an extension of a potential window by about 100 mV can be achieved by replacing PNP^+ by TDA^+ in o-DCB. Hence o-DCB is a promising non-aqueous solvent for the studies of a large number of ions.

Ac cyclic voltammetry have been used for the determination of the standard Galvani potential difference and the standard Gibbs energy of partition of anions and cations in water/o-DCB system. The standard Gibbs energies of transfer of the ions $TPAs^+$, TBA^+, TPP^+ and TPB^- have also been determined from solubility experiments. The values obtained from solubility experiments have been found to be in good agreement with the values obtained from voltammetry.

Electrical double layer studies for the system LiCl in water and PNPDCC in o-DCB have shown that there is an extensive ion association in the organic phase. Unlike the water/nitrobenzene and water/1,2-dichloroethane systems the potential of the capacitance minimum of the water/o-DCB is found to be more negative. Hence further studies are necessary to better understand the structure of the water/o-DCB interface.

R E F E R E N C E S

1. W. Nernst and E.H. Riesenfeld, Ann. Phys., 8(1902)60
2. K.F. Bonhoeffer, and H. Sterehlow, Z. Elektrochem., 57(1953)614, Chem. Abstr., 48(1953)56870.
3. F.M. Karpfen and J.E.B. Randels, Trans. Faradays Soc., 49(1953)823.
4. J. Guastalla, C.R. Acad. Sci. Ser. C., 269(1969)1360, Chem. Abstr., 72(1970)47760z.
5. J. Guastalla and C. Bertrand, C.R. Acid. Sci. Ser. C., 274(1972)1884. Chem. Abstr., 77(1972)108722r.
6. M. Blank, J. Colloid interface Sci., 22(1966)51. Chem. Abstr., 65(1966)97736.
7. B. D Epenoux and C. Gavach, J. Colloid Interface Sci., 56(1976)138. Chem. Abstr. 85(1976)130998x.
8. C. Gavach and B.D. Epenoux, C.R. Acad. Sci. Ser. C., 272(1971)872., Chem. Abstr., 74(1971)150236y.
9. P. Joos and M. Van Bockstaele, J. Phys. Chem., 80(1976)1573.
10. P. Joos and R. Vanden Bogaert, J. Colloid Interface Xci., 56(1976)206., Chem. Abstr., 85(1976)99568f
11. J. Koryta, J. Electrochim Acta, 24(1979)293.
12. J. Koryta, J. Electrochim Acta, 29(1984)445.
13. J. Koryta, J. Electrochim Acta, 32(1987)419.
14. J. Koryta, J. Electrochim Acta, 33(1988)189.
15. J. Koryta, and P. Vanysek, Electrochemical Sciences

15. J. Koryta, and P. Vanysek, Electrochemical phenomena at at the Interface of two Immiscible Electrolyte Solutions, in Advances in Electrochemistry and Electrochemical Engineering, Vol. 12(Ed. by H. A. Gerisher and C.W. Tobias) pp. 113-176. Wiley-Interscience, New York (1981).

16. P. Vanysek and R.P. Buck, J. Electroanal. Chem., 163(1984)1.

17. H.H. Girault and D.J. Shiffrin, Electrochemistry of liquid/liquid Interfaces, South Ampton, England, 1986.

18. P. Bonysek, Electrochemistry on liquid/liquid Interface, in Lecture Notes in Chemistry, Spinger-Verlag, Berlin, 1985.

19. C. Gavach, F. Henry J. Elecroanal. Chem., 54(1974)361.

20. C. Gavach, and B.D. Epenoux, J. Electroanal. Chem. 55(1974)59.

21. C. Gavach, F. Henry and B.D. Penoux, J. Electroanal. Chem., 64(1975)107.

22. J. Koryta, P. Vanysek and M. Brexina, J. Electroanal. Chem., 67(1976)263.

23. J. Koryta, P. Vanysek and M. Brezina, J. Electroanal. Chem., 75(1977)211.

24. Z. Somec, J. Koryta and M.W. Khalil, J. Electroanal. Chem. 83(1977)393.

25. Lo.Q. Hung, Z. Samec, V. Marecek, J. Weber and D. Homolka, J. Electroanal. Chem., 99(1979)385.

26. D. Homolka, Lo.Q. Hung, A. Hofmanova. M.W. Khalil, J. Koryta, V. Marecek, Z. Samec, D.K. Drn, P. Vanysek, M. Brezina, M. Jsnfs, snf I. Dyibor, Anal. Chem. 52(1980)1606.

27. D. Homolka and P. Vanysek, J. Electroanal. Chem. 112(1980)91.

28. R.P. Buck, Ion-Select.ElectroRev., 4(1982)3. Chem. Abstr. 97(1982)152872b.

29. V. Marecek and Z. Samec, J. Electroanal. Chem., 149(1983)185.

30. V. Marecek and Z. Samec, J. Electroanal. Chem., 185(1985)268. Soc. 77(1984)187.

31. Z. Samec, V. Marecek, D. Homolka, Farady Disc, Chem., Soc. 77(1984)187.

32. T. Solomon, H. Alemu, B. Hundhammer, J. Electroanal. Chem., 169(1984)303.

33. O. Valent, J. Koryta, and M. Panoch, J. Electroanal. Chem., 226(1987)21.

34. H. Alemu and T. Solomon, J. Electroanal. Chem., 23 237(1987)113.

35. S. Kihara, M. Suzuki, K. Maeda, K. Ogura, S. Umentani, M. Matsui, and A. Yoshia, anal. Chem., 58(1986)2954.

36. H. Alemu, T. Solomon, J. Electroanal. Chem., 261(1989)261.

37. Z. Somec, D. Homolka, V. Marecek and L. Kavan, J. Electroanal. Chem., 145(1983)213.

38. I. Paleska, J. Kotowski, Z. Koczorowski, E. Nakache, and M. Dupeyrat, J. Electroanal. Chem., 278(1990)129.

39. T. Solomon H. Alemu and B. Hundhammer, J. Electroanal. Chem., 169(1984)311.

40. Z. Kiczorowski, G. Geblewicz, and I. Paleska, J. Electroanal. Chem., 172(1984)327.

41. S. Kihara, M. Suzuki, K. Maeda, K. Ogura, and M. Matsui, J. Electroanal. Chem., 210(1986)147.

42. B. Hundhammer and S. Wilke, J. Electroanal. Chem., 266(1989)133.

43. Z. Samec, Chem. Rev., 88(1988)617.

44. J. Rais, Collect Czech. Chem. Commun., 36(1971)3253.

45. J. Koryta, M. Brezina, A. Hofmanova, D. Homolka, S.K. Sen. P. Vanysek, and J. Weber, Bioelectrochem. Bioenerg., 7(1980)61, Chem. Abstr., 93(1980)90244e

46. J. Czapkiewicz, Czapkiewisz, Tutaj, J. Chem. Soc. Faraday Trans. I, 76(1980)1663.

47. M.H. Abraham and A. Daniel de Namor, J. Chem. Soc. Faraday Trans. I, 72(1976)955.

48. Y. Marcus, Pure Appl. Chem., 55(1983)977.

49. C. Gavach, P. Seta, and B.D. Epenoux, J. Electroanal. Chem., 83(1977)225.

50. H.H. Giraut, D.J. Shiffrin, J. Electroanal. Chem., 150(1983)43.

51. Z. Samec, V. Marecek, D. Homolka, J. Electroanal. Chem., 187(1985)31.

52. G.M. Torrie, J.D. Valleau, J. Electroanal. Chem., 206(1986)69.

53. Z. Samec, V. Marecek, J. Weber, J. Electroanal. Chem., 100(1979)841.

54. T. Osakai, T. Kakutami, M. Senda, Bull. Chem. Soc. Jpn., 57(1984)370.

55. O.R. Melroy, W.E. Bronner, R.P. Buck, J. Electroanal. Chem., 130(1983)373.

56. Z. Samec, V. Marecek, J. Electroanal. Chem., 200(1986)17.

57. A.M. Baruzzi and J. Uhlken, J. Electroanal. Chem., 282(1990)267.

58. M. Gros, S. Gromb, C. Gavach, J. Electroanal. Chem., 80(1978)29.

59. J.D. Reid, O.R. Melroy, R.P. Buck, J. Electroanal. Chem., 147(1983)71.

60. T. Kakiuchi, M. Senda, Bull. Chem. Soc. Jpn., 56(1983)1753.

61. T. Kakiuchi, M. Senda, Bull. Chem. Soc. Jpn. 56(1983)1322.

62. H.H. Girault and D.J. Shiffrin, J. Electroanal. Cgem., 170(1984)127.

63. G. Gelewicz, Z. Figaszewski, Z. Koczorowski, J. Electroanal. Chem., 177(1984)1.

64. F. Silva, C. Moura, J. Electroanal. Chem., 177(1984)317.

65. D.J. Reid, P. Vanysek, R.P. Buck, J. Electroanal. Chem., 170(1984)109.

66. S. Chechirlian, P. Eichner, M. Keddam, H. Takenouti and H. Mazille, J. Electrochim Acta, 35(1990)1125.

67. Z. Samec,,V. Marecek, K. Holub, S. Racinsky, P. Hajkova, J. Electroanal. Chem., 225(1987)65.

68. P. Hajkova, D. Homolka, V. Marecek, Z. Samec, J. Electroanal. Chem., 151(1983)277.

83. T. Shedlovsky, J. Frauklin Ist. 225(1938)739; Chem. Abstr. 32(1938)8888[2]

84. J.I.Kim, Z. Phys. Chemic. Frankfurt, 113(1978)151; Chem. Abstr. 88(1978)66493m.

85. CRC Handbook of Chemistry and Physics, CRC Press Inc. 1988.

86. B.S. Krumgalz, J. Chem. Soc. Faraday Trans. I., 79(1983)571.

87. W.R. Gilkerson, J. Chem. Phys. 25(1956)99.

88. R.M. Fuess, J. Amerr Chem. Soc., 80(1958)5059.

89. E. Grunwald, G. Daughman and G. Kohanslan, J. Amer. Chem. Soc., 82(1966)5801.

90. B. Hundhammer and T. Solomon, J. Electroanal. Chem., 157(1983)19.

D E D I C A T I O N

To my father - Haji Hassen Ahmed

To my mother - W/o Fatima Seid

and

To my daughter - Rosa